

NMSSM Higgs boson self-couplings at next-to-leading order

Diplomarbeit
von

Juraj Streicher

An der Fakultät für Physik
Institut für Theoretische Physik

Referent: Prof. Dr. M. Mühlleitner
Korreferent: Prof. Dr. M. Steinhauser

Juni 2012

Ich versichere, dass ich diese Arbeit selbstständig verfasst und ausschließlich die angegebenen Hilfsmittel verwendet habe.

Juraj Streicher
Karlsruhe, den 04. Juni 2012

Als Diplomarbeit anerkannt.

Prof. Dr. M. Mühlleitner
Karlsruhe, den 04. Juni 2012

Deutsche Zusammenfassung

Das Standardmodell der Teilchenphysik ist eine Theorie, die es in den letzten Jahrzehnten mit Bravour geschafft hat, eine überwältigende Mehrheit der Beobachtungen auf dem Gebiet der Elementarteilchenphysik in einer spontan gebrochenen Quantenfeldtheorie zusammenzufassen. Darüber hinaus trifft sie Vorhersagen über noch zu entdeckende Teilchen, basierend lediglich auf der Annahme, dass die zu Grunde liegende Theorie der Natur Symmetrien aufweist. So ist es zum Beispiel Makoto Kobayashi and Toshihide Maskawa bereits 1973 gelungen, das Top-Quark vorherzusagen, das 22 Jahre später am Tevatron experimentell nachgewiesen werden konnte.

Heute wie vor 20 Jahren ist das Standardmodell einer schweren Bewährungsprobe gestellt, da der 2009 angelaufene Large Hadron Collider (LHC) es sich zum erklärten Ziel gesetzt hat, das letzte bisher unbeobachtete Teilchen des Standardmodells, das Higgs-Boson, nachzuweisen. Der LHC und seine Experimente ATLAS und CMS wurden so konzipiert, dass sie die Frage, ob es ein Higgs-Boson wie es das Standardmodell vorhersagt gibt oder nicht, eindeutig beantworten können.

Die am LHC anfangs gesammelten Daten haben sukzessiv den erlaubten Massenbereich für das Higgs-Boson verkleinert. Obwohl dies ein erwartetes Verhalten war, da die theoretischen und experimentellen Einschränkungen des Standardmodells ein leichtes Higgs-Boson präferieren, der LHC in diesem Massenbereich jedoch eine geringere Signifikanz aufweist, gab dies Anlass zu bedenken, denn die gesamte Theorie der elektroschwachen Wechselwirkung, welche in den vergangenen Jahren ausgiebig in Präzisionstests untersucht und bestätigt wurde, beruht auf der Existenz eines Higgs-Bosons. Theorien mit erweiterten Higgs-Sektoren bieten für den Fall dass das Standardmodell Higgs-Boson von den LHC-Experimenten ausgeschlossen werden sollte, eine Lösung der daraus entstehenden Probleme, so dass das Standardmodell weiterhin als effektive Theorie seine Gültigkeit bewahrt. Das Ziel dieser Arbeit war es, ein mögliches Szenario, in dem das standardmodellartige Higgs-Boson experimentell ausgeschlossen werden würde, im Rahmen der Nächst-minimalen Supersymmetrischen Erweiterung des Standardmodells (NMSSM) zu diskutieren.

Supersymmetrische Erweiterungen des Standardmodells benötigen per se einen erweiterten Higgs-Sektor und eignen sich somit, um das eventuelle Nichtvorhandensein des erwarteten Higgs-Signals zu erklären. Die Grundidee hinter diesen Erweiterungen ist es jedoch, die Willkür zwischen den bosonischen und fermionischen Teilchen durch eine zusätzliche Symmetrie der Natur zu lösen: alle Felder des Standardmodells werden zu Superfeldern erweitert, welche neben den bereits bekannten Teilchen zusätzliche Freiheitsgrade mit komplementärem Spin aufweisen. So werden in der NMSSM die fermionischen Felder der Leptonen und Quarks um je zwei¹ bosonische Spin-0-Felder der Sleptonen und Squarks, ergänzt, während die Eichbosonen der starken Wechselwirkung, die Gluonen, jeweils einen fermionischen Spin-1/2-Superpartner namens Gluino erhalten.

¹Eine Ausnahme bilden hier die Neutrinos, die im Rahmen des Standardmodells als masselos behandelt werden, deswegen einen Freiheitsgrad weniger und damit auch nur ein skalares Superpartner-Feld besitzen.

Der skalare Higgs-Sektor der NMSSM ist verglichen zum Standardmodell um ein zweites Higgs-Dublett erweitert, welches allgemein in supersymmetrischen Theorien benötigt wird um Quarkmassen zu generieren, und um ein drittes Higgs-Feld², welches ein Singlett unter der Eichgruppe ist und somit nicht an die Felder des Standardmodells koppelt. Die Superpartner dieser Higgs-Felder mischen zusammen mit den Superpartnern der elektroschwachen Eichbosonen und formen die fermionischen Masseneigenzustände der Neutralinos und Charginos. Somit umfasst das Teilchenspektrum der NMSSM neben den Teilchen des Standardmodells zwei weitere skalare, zwei pseudoskalare und zwei geladene Higgs-Bosonen, neun Sleptonen, zwölf Squarks, acht Gluinos, fünf Neutralinos und zwei Charginos.

Die Tatsache, dass bislang keines dieser supersymmetrischen Partnerteilchen experimentell nachgewiesen wurde, wird in der Theorie durch eine explizite Brechung der Supersymmetrie erklärt. Diese sorgt dafür, dass die Massen der Superpartner nicht identisch sind, wie von exakter Supersymmetrie verlangt wäre.

Der erweiterte Higgs-Sektor der NMSSM ergibt etliche Konsequenzen für die Higgs-Suche am LHC. Zum Einen führen die Beiträge des Higgs-Singletts in den Higgs-Boson-Masseneigenzuständen zu einer Unterdrückung der Kopplungen an Standardmodell Teilchen, wodurch die Produktions- und Zerfallswirkungsquerschnitte der Higgs-Bosonen verringert werden.

Zum Anderen kann in der NMSSM das leichteste Higgs-Boson pseudoskalar sein, für welches die Ausschlussgrenzen der direkten Higgs-Suche am LEP nicht anwendbar sind und das demnach dominant in Bottom-, oder gar leichtere, Quarks zerfallen könnte. Szenarien dieser Art wurden in der Vergangenheit ausgiebig untersucht und zeigten, dass für große Bereiche des NMSSM-Parameterraums keines der Higgs-Bosonen durch die gängigen LHC-Higgs-Entdeckungskanäle gefunden oder ausgeschlossen werden könnte. In dieser Arbeit wird der Einfluss von Korrekturen der nächst-zur-führenden Ordnung zu dem Zerfall der skalaren Higgs-Bosonen, h_i , in die leichtesten pseudoskalaren, A_1 , untersucht.

Der herausforderndste Teil dieser Aufgabe war die Renormierung der Higgs-Kopplung, da auf Ein-Schleifen-Niveau über 2000 Diagramme zu diesem Prozess beitragen, was, zusammen mit der Komplexität der NMSSM-Kopplungen, eine analytische Behandlung der Renormierungsprozedur unmöglich macht. Die Ein-Schleifen-korrigierte Amplitude wurde deswegen in der Feynman-Graphen-Methode mit den Mathematica-Paketen `FeynArts` und `FormCalc`, zusammen mit Zuhilfenahme von eigens geschriebenen `Bash` und `Form` Routinen aufgestellt. Die Gesamtamplitude folgte daraus als Summe der im Allgemeinen divergenten Passarino-Veltmann-Integrale gewichtet mit generischen Vertexfunktionen und weiteren Parametern der NMSSM. Diese wurden numerisch mit `LoopTools` und weiteren Mathematica-Routinen ausgewertet. Um die Renormierung zu vollenden, musste zusätzlich der Counterterm zu der trilinearen Higgs-Selbstkopplung bestimmt werden, der die divergenten Anteile der Ein-Schleifen-Amplitude ausgleicht und, abhängig von dem Renormierungsschema, eventuell zusätzliche endliche Beiträge zu der Korrektur liefert. Hierzu wurden die von der Arbeitsgruppe von Prof. M. Mühlleitner entwickelten Mathematica-Programme zur numerischen Bestimmung der Renormierungskonstanten des NMSSM Higgs-Sektors benutzt, die letztendlich zu einer numerischen Aufhebung der divergenten Anteile der Ein-Schleifen Amplitude und des zugehörigen Counterterms mit einer Präzision von 10^{-10} geführt haben. Diese Programme erlauben zusätzlich eine Einschätzung des theoretischen Fehlers, der durch das Vernachlässigen höherer Ordnungen der Störungsrechnung entsteht, indem das Renormierungsschema für die Bestimmung der Top- und Bottom-Quarkmassen variiert wird. Die Analyse der gefundenen Szenarien wurde deswegen sowohl für Pol-Quarkmassen durchgeführt, als auch für laufende $\overline{\text{DR}}$ Top- und Bottom-Quarkmassen durchgeführt.

²Dieses Higgs-Singlett ist der Grund für die Namensgebung der NMSSM. Wenn man es nicht einführt, bildet der Feldinhalt eine Minimalmenge von Feldern, die für eine supersymmetrische Erweiterung des Standardmodells benötigt werden.

Die hieraus resultierende Ein-Schleifen-korrigierte Higgs-Selbstkopplung wurde auf ihren phänomenologischen Einfluss untersucht, dabei wurde der veränderte Stand der Higgs-Suche am LHC berücksichtigt. Im Laufe des vergangenen Jahres haben sowohl ATLAS als auch CMS bestätigt, eine Higgs-Boson Evidenz mit einer lokalen statistischen Signifikanz von 3.5σ , beziehungsweise 3.1σ im Massenbereich um 125 GeV registriert zu haben. Wenn sich diese Evidenz nicht zu einer statistischen Schwankung entwickelt, ist damit zu rechnen, dass die Higgs-Boson Entdeckung bis zum Ende des Jahres 2012 bestätigt werden kann.

Diese Evidenz bildet keine ideale Basis für die ursprünglich angedachte Analyse, weswegen die Szenariensuche für die Auswertung angepasst werden musste. Betrachtet wurden letztendlich Parameterpunkte, die ein Signal produzieren, welches mit der gemessenen Signifikanz eines standardmodellartigen Higgs-Bosons im Massenbereich um 125 GeV übereinstimmen. Da ein solches Signal nur erzeugt werden kann, wenn die Verzweungsverhältnisse des standardmodellartigen Higgs-Bosons nicht durch zusätzliche Zerfallskanäle merklich beeinflusst werden, konzentriert sich die Untersuchung auf die Auswirkungen der korrigierten Selbstkopplung zwischen den nicht-standardmodellartigen und den leichtesten pseudoskalaren Higgs-Bosonen.

Zu diesem Zweck wurde ein Programm geschrieben, welches den Parameterraum des NMSSM Higgs-Sektors nach Punkten gescannt hat, die ein leichtes pseudoskalares A_1 und ein standardmodellartiges Higgs-Boson mit einer Masse um 125 GeV aufweisen. Nach diesen Kriterien wurden über 500000 zufällige Parameterpunkte gescannt und bei den potentiell interessanten Punkten wurde der Einfluss der korrigierten Selbstkopplung auf die resultierenden Zerfallsbreiten untersucht.

Die meisten so gefundenen Punkte weisen größtenteils Korrekturen von weniger als 20% auf, ein repräsentatives Beispiel für solche Szenarien wird in Kapitel 6.3 geschildert. Es wurden vereinzelt auch Szenarien gefunden, in denen die Korrektur erhebliche Auswirkungen auf die Phänomenologie hat, wie man dem in Kapitel 6.4 diskutierten Szenario entnehmen kann. Dieses erfüllt jedoch nicht das erforderliche Kriterium der standardmodellartigen Verzweungsverhältnisse, zeigt aber dennoch, dass die Ein-Schleifen-Korrekturen zu der Higgs Selbstkopplung durchaus nicht zu vernachlässigen sind.

Aus den ausgewerteten Daten lässt sich eine Tendenz ablesen, derzufolge in Szenarien mit standardmodellartigen Higgs-Bosonen mit einer Masse um 125 GeV die betrachteten Ein-Schleifen-Korrekturen klein ausfallen, eine eindeutige Aussage bedarf jedoch weiterer Untersuchungen. Die in dieser Diplomarbeit erzielten Ergebnisse dienen als Grundlage für weiterreichende Projekte, in denen die Korrekturen zu der CP-verletzenden Higgs-Selbstkopplung bestimmt und diese in eine modifizierte Version von HDECAY eingepflegt werden, die es dadurch erlaubt, NMSSM-Higgs-Zerfälle auf Ein-Schleifen-Niveau berechnen zu können.

In der nachfolgenden Diplomarbeit wird die hier zusammengefasste Analyse der Ein-Schleifen-Korrekturen zur Selbstkopplung der NMSSM Higgs-Bosonen ausführlicher diskutiert. In Kapitel 2 werden Grundlagen der Quantenfeldtheorie präsentiert und benutzt, um die Lagrange-Dichte des Standardmodells herzuleiten.

Das Kapitel 3 bietet eine kurze Einführung in das Konzept der Supersymmetrie und schildert, wie supersymmetrische Theorien manche Makel des Standardmodells lösen können. Des Weiteren wird in diesem Kapitel das Teilchenspektrum der NMSSM vorgestellt und das damit einhergehende Higgs-Potential im Detail diskutiert, woraus die für die Higgs-Phänomenologie erforderlichen Parameter abgeleitet werden.

Die grundsätzlichen Konzepte und technischen Einzelheiten der Renormierung, die man für die Berechnung der Ein-Schleifen-Korrekturen der Higgs Selbstkopplung benötigt, werden im Kapitel 4 eingeführt.

Anschließend werden die zuvorgehenden Grundlagen im Kapitel 5 zusammengefügt, um die Ein-schleifen-korrigierte Zerfallsbreite des skalaren Higgs-Bosons h_i in zwei leichte pseudoskalare A_1 zu berechnen.

Die phänomenologischen Auswirkungen dieser Korrektur werden an den bereits erwähnten Beispielen von zwei Szenarien ausführlich in Kapitel 6 präsentiert.

Contents

1. Introduction	1
2. Quantum Field Theory and the Standard Model	3
2.1. Quantum Field Theory	3
2.2. The Lagrangian and its Symmetries	3
2.3. The Standard Model Gauge Group	4
2.4. The Higgs Mechanism	5
2.5. Flaws of the Standard Model	6
3. Supersymmetry and the NMSSM	9
3.1. The Concept of Supersymmetry	9
3.2. Solutions provided by Supersymmetry	10
3.3. Passing the MSSM	11
3.4. The Lagrangian of the NMSSM	12
3.5. The Scalar NMSSM Higgs Potential	14
3.5.1. Neutral Higgs Boson Mass Matrix	15
3.5.2. Charged Higgs Boson Mass Matrix	16
4. Introduction to Renormalisation	19
4.1. Of Loops and Infinities	20
4.2. The Concept of Renormalisation	21
4.3. General Renormalisation Procedure	22
4.3.1. Methods of Regularisation	22
4.3.2. Counterterm Formalism	23
4.3.3. Renormalisation Conditions	24
4.3.4. Renormalisation Schemes	25
5. Higgs Vertex Renormalisation	27
5.1. Loop Diagrams	27
5.1.1. Crosschecks	29
5.2. Counterterms	29
5.2.1. Parameter Basis	29
5.2.2. Renormalisation Conditions	30
5.2.3. Vertex Renormalisation Contributions	32
5.2.4. Field Renormalisation Contributions	32
5.3. Z and Goldstone Boson Transitions	33
5.4. Mass Corrections	34
6. Numerical Analysis	37
6.1. Scenario Search	37
6.2. Parameter Scan Procedure	38
6.3. Scenario 1	40

6.4. Scenario 2	43
7. Conclusion	49
A. Trilinear Higgs Self-Coupling	51
B. The Decay Width	53
References	55

This thesis was written in a very exciting year for the particle physicists community, as the Large Hadron Collider (LHC) has achieved notable progress in its aim to probe the fundamental laws of nature beyond the electroweak scale. One of the main design features of the LHC and its general purpose detector experiments ATLAS and CMS is their discovery potential [1] for the last heretofore unobserved particle predicted by the Standard Model, the Higgs boson. This design feature is sometimes referred to as the no-lose theorem, as according to theoretical constraints of the Standard Model [2], the Higgs boson mass must lie below 800 GeV and therefore, if the Standard Model is to remain a valid description of elementary particle physics at the electroweak scale, it is simply a matter of time, until it will be discovered at the LHC.

Ever since the LHC began operation in the late 2009, experimental data have been continually accumulated and evaluated, narrowing the allowed mass region for the Standard Model Higgs increasingly. This trend was not surprising, as the theoretical and experimental constraints on the Standard Model prefer a light Higgs boson, for which the significance of the LHC experiments is limited, but still the trend has encouraged to investigate the questions, about how electroweak symmetry breaking, required by the Standard Model, could be achieved, in case the LHC excludes the Standard Model Higgs boson. The Next-to-Minimal Supersymmetric Extension of the Standard Model (NMSSM) considered in this thesis, offers a sophisticated way to resolve such potential issues. The NMSSM Higgs sector introduces two additional scalar Higgs bosons h_i , as well as further two pseudoscalar, A_i , and two charged Higgs bosons H^\pm and thus yields an enriched Higgs boson phenomenology, to which the Standard Model no-lose theorem does not apply.

The efforts to formulate a no-lose theorem for the NMSSM Higgs boson search at the LHC up to now were in vain, as large parameter space regions yield the lightest Higgs boson to be the pseudoscalar A_1 so that the potential Standard Model-like scalar Higgs boson could decay dominantly into these pseudoscalars, thereby escaping detection in the standard LHC Higgs search channels. Thus, in the light of these circumstances, it was an interesting question to ask, what phenomenological impact one-loop corrections to the Higgs boson self-couplings would yield in scenarios, where no Standard Model-like Higgs is found on the entire mass range due to the presence of the $h_1 \rightarrow A_1 A_1$ decay channel.

The initial motivation for the analysis of the one-loop corrected Higgs-to-Higgs decays performed in this thesis, however, had to be reconsidered due to recent development in the LHC

Higgs search, as in the late 2011 both ATLAS and CMS experiments announced a Higgs boson evidence with a local statistical significance of 3.5σ and 3.1σ respectively in the mass region around 125 GeV, predicting that if this evidence is not a mere statistical fluctuation, the Higgs boson is likely to be discovered with 5σ confidence level in 2012. While this announcement has no effect on the validity of the actual calculations performed in this thesis, the phenomenological discussion of the consequences of these calculations had to be rethought.

In the following chapter 2 a few general remarks about quantum field theories are made. These are then applied to construct the Lagrangian of the Standard Model.

Chapter 3 provides a brief introduction to the concept of Supersymmetry and a discussion on how supersymmetric extensions can be used to solve certain flaws of the Standard Model. The particle spectrum of the NMSSM is introduced and resulting the Higgs sector is discussed in detail, defining quantities and parameters required for calculations of the NMSSM Higgs phenomenology.

The fundamental concepts and technical aspects of renormalisation required for calculations of higher order corrections are presented in chapter 4.

All these preliminary remarks are assembled in chapter 5 which provides a description on how the one-loop corrected amplitude for the decay of a scalar Higgs boson h_i into two pseudoscalar Higgs bosons A_1 is calculated in the Feynman diagrammatic approach.

Ultimately, the phenomenological consequences of the inclusion of one-loop corrections to the Higgs decay widths are examined in chapter 6.

Quantum Field Theory and the Standard Model

2.1. Quantum Field Theory

In the beginning of the 20th century, milestones in physics were set by the formulation of special relativity and quantum mechanics, which extended the classical laws of physics to domains, where velocities are comparable with the speed of light, and to length scales comparable to the atomic radii respectively. Questions arose subsequently about how to describe the realm of elementary particle physics, where effects of these both theories have to be taken into account simultaneously. The answer to these questions was soon after found in *quantum field theory*, which ingeniously incorporates the requirements for *Poincaré invariance*, which is necessary for conservation of energy and momentum, the *uncertainty principle* demanded by quantum mechanics and *cluster decomposition* which states that spacelike separated events yield uncorrelated results.

By additionally including the concept of *renormalisation* - a mathematical statement that a model is not the ultimate theory describing all of nature's laws - the physicists of the past century have managed to construct a quantum field theory called the *Standard Model*, which describes the majority of known phenomena of nature¹ with remarkable precision.

2.2. The Lagrangian and its Symmetries

The fundamental mathematical framework for describing a quantum field theory is expressed by the Lagrangian density $\mathcal{L}(\varphi, \partial_\mu\varphi)$, a local function of fermionic and bosonic quantum fields and their spacetime derivatives, which is connected with the action S via,

$$S = \int d^4x_\mu \mathcal{L}(\varphi, \partial_\mu\varphi).$$

A reason for this choice can be seen within the established general strategy of expressing equations of motion in terms of conserved quantities such as momentum, or charge. According to Noether's theorem, conserved quantities are associated with the invariance of the action S under a continuous transformation of the fields or coordinates of \mathcal{L} . Apart from symmetries

¹Since the effect of gravitation is negligibly small compared to the electroweak and strong interactions, it is not included in the Standard Model.

under Lorentz boosts and rotations plus spacetime translations generated by the Poincaré group, quantum field theories can also be invariant under internal gauge transformations of the fields. In the most general case such transformations are local $SU(N)$ gauge symmetries of N fermionic fields $\psi_i(x)$ arranged to a multiplet $\Psi(x)$,

$$\Psi(x) \rightarrow U\Psi(x) = e^{i\lambda^a(x)T^a} \Psi(x), \quad \Psi(x) = (\psi_1(x), \dots, \psi_N(x))^T, \quad (2.1)$$

where T^a are the group generators² and $\lambda^a(x)$ are $N^2 - 1$ spacetime functions. The kinetic part of the Lagrangian is invariant under gauge transformation only when the usual derivative ∂_μ is replaced in a covariant form involving $N^2 - 1$ gauge fields $A_\mu^a(x)$. These gauge fields couple to the fermionic multiplet $\Psi(x)$ with the coupling strength g and transform under the adjoint representation,

$$\partial_\mu \rightarrow \mathcal{D}_\mu = \partial_\mu - igA_\mu^a(x)T^a. \quad (2.2)$$

The kinetic term of the gauge fields is proportional to the square of the field strength tensor $F_{\mu\nu}$ defined as,

$$F_{\mu\nu}^a T^a = \frac{i}{g} [\mathcal{D}_\mu, \mathcal{D}_\nu]. \quad (2.3)$$

Thus, defining the field content in a way that all elemental particles can be described as excitations of those fields, and demanding renormalisability as well as symmetry of \mathcal{L} under certain transformations due to the conservation of the related quantities leads to the general form of the Lagrangian.

2.3. The Standard Model Gauge Group

The Standard Model successfully combines all known elementary particles and three of the four observed forces of nature into a spontaneously broken gauge theory. The Lagrangian of this quantum field theory is symmetric under transformations of a non-abelian group represented by the tensor product

$$SU(3)_C \otimes SU(2)_L \otimes U(1)_Y, \quad (2.4)$$

where $SU(3)_C$ is the symmetry group of the strong force between quarks, with gluons as interaction mediators and associated conservation of the colour charge. The phenomenology of strongly interacting particles is fully described by quantum chromodynamics. [3, 4]

The remaining $SU(2)_L \otimes U(1)_Y$ symmetry is associated with the conservation of the weak isospin (respectively its component I_3) and hypercharge³ Y and builds the fundamentals of the phenomenology of the electromagnetic and weak interactions unified within the Glashow-Weinberg-Salam electroweak theory. [5, 6]

All heretofore observed elementary particles can be classified within the Standard Model into chiral right-handed singlets and left-handed doublets according to their transformation behaviour under the symmetry group Eq. (2.4) as stated in Tab. 2.1.

²The generators of the $SU(2)$ and $SU(3)$ groups are proportional to the Pauli matrices σ^a and to the Gell-Mann matrices λ^a respectively.

³In the process of electroweak symmetry breaking these quantities lead to the conservation of electric charge Q given by the Gell-Mann-Nishijima formula: $Q = I_3 + Y$.

Field				SU(3)	SU(2)	U(1)
Q_L^i	$(u_L, d_L)^T$	$(c_L, s_L)^T$	$(t_L, b_L)^T$	3	2	1/6
u_R^i	u_R	c_R	t_R	3	1	2/3
d_R^i	d_R	s_R	b_R	3	1	-1/3
L_L^i	$(\nu_{e,L}, e_L)^T$	$(\nu_{\mu,L}, \mu_L)^T$	$(\nu_{\tau,L}, \tau_L)^T$	1	2	-1/2
l_R^i	e_R	μ_R	τ_R	1	1	-1
Φ	$(\phi^+, \phi^0)^T$			1	2	1/2

Table 2.1.: Matter field content of the Standard Model with corresponding gauge quantum numbers. The fermionic quark and lepton fields Q_L^i , L_L^i , u_R^i , d_R^i , l_r^i exist in three generations $i = 1, 2, 3$ distinguished solely by the mass of the particles, whereas only one bosonic Higgs doublet Φ is required.

Right-handed neutrinos, while not forbidden by theoretical arguments, are not included in the Standard Model, as they transform as singlets under the gauge group Eq. (2.4) and therefore couple to none of the force mediators.

Additionally to the matter fields, one gauge field for every generator of the symmetry group has to be included in the theory. These are the 8 gluon fields G_μ^a for the strongly interacting sector and 4 fields W_μ^1 , W_μ^2 , W_μ^3 , B_μ for the electroweak sector, so that the kinetic part of the Lagrangian \mathcal{L} ,

$$\mathcal{L}_{\text{kin}}^{\text{F}} = i\bar{\psi}\not{\partial}\psi, \quad \psi = Q_L^i, u_R^i, d_R^i, L_L^i, l_R^i \quad (2.5)$$

with $\mathcal{D}_\mu = \partial_\mu - ig_s \frac{\lambda_a}{2} G_\mu^a - ig_2 \frac{\sigma_a}{2} W_\mu^a - ig_1 Y B_\mu$

remains invariant under gauge transformations. These fields correspond to the mediator fields of the interactions. Gauge invariant couplings between matter and mediator fields are generated dynamically from the kinetic term, whereas eventual self-interactions among the gauge fields result from the gauge-kinetic part of \mathcal{L}

$$\mathcal{L}_{\text{kin}}^{\text{G}} = -\frac{1}{4}(G_{\mu\nu}^a G^{a\mu\nu} + W_{\mu\nu}^a W^{a\mu\nu} + B_{\mu\nu} B^{\mu\nu}) \quad (2.6)$$

where $G_{\mu\nu}^a$, $W_{\mu\nu}^a$, and $B_{\mu\nu}$ are the field strength tensors defined by Eq. (2.3).

2.4. The Higgs Mechanism

Complications arise, when the particles in a gauge theory are to have a non-zero mass, as the usual Lorentz invariant mass terms quadratic in the fields are not gauge invariant. In the Standard Model this problem is solved by the Higgs mechanism [7–10] by adding a complex scalar doublet field Φ with quantum numbers as presented in the last line of Tab. 2.1. When the Higgs field potential is constructed as

$$V_{\text{Higgs}} = \mu^2 \Phi^\dagger \Phi + \frac{\lambda}{4} |\Phi^\dagger \Phi|^2 \quad (2.7)$$

with $\mu^2 < 0$ and $\lambda > 0$, it possesses a non-vanishing vacuum expectation value which, in the special choice of unitary gauge, reads

$$\langle \Phi \rangle = (0, v/\sqrt{2})^T.$$

Where v is related to the Fermi constant G_F as $v = (\sqrt{2}G_F)^{-1/2}$ and thereby experimentally determined to be $v = 246\text{GeV}$. The electroweak symmetry breaking (EWSB) emerges from the minimisation of the Higgs field, as its contribution to the kinetic part of the Lagrangian,

$$\mathcal{L}_{\text{kin}}^{\text{H}} = (\mathcal{D}_\mu \Phi)^\dagger (\mathcal{D}^\mu \Phi) \xrightarrow{\text{EWSB}} \frac{v^2}{8} [g_2^2 (W_\mu^1 + iW_\mu^2)(W_\mu^1 - iW_\mu^2) + (g_2 W_\mu^3 - g_1 B_\mu)^2], \quad (2.8)$$

yields mass terms for physical combinations of the gauge fields. These are the neutral photon A_μ , the massive Z -boson Z_μ and the charged W -bosons W_μ^\pm . With the Weinberg angle $\cos \theta_W = g_2/\sqrt{g_1^2 + g_2^2}$, these can be written in terms of the gauge fields as

$$\begin{aligned} W_\mu^\pm &= \frac{1}{\sqrt{2}} (W_\mu^1 \mp iW_\mu^2), & \text{with } m_W &= \frac{g_2 v}{2} \\ Z_\mu &= \cos \theta_W W_\mu^3 - \sin \theta_W B_\mu, & \text{with } m_Z &= \frac{v \sqrt{g_1^2 + g_2^2}}{2} \\ A_\mu &= \sin \theta_W W_\mu^3 + \cos \theta_W B_\mu, & \text{with } m_\gamma &= 0. \end{aligned}$$

Gauge invariant fermion mass terms can likewise be included in the Lagrangian as Yukawa couplings between the fermion fields and the Higgs field⁴,

$$\begin{aligned} \mathcal{L}_{\text{mass}}^{\text{F}} &= \mathcal{L}_y^{\text{F}} + h.c. & (2.9) \\ \mathcal{L}_y^{\text{F}} &= Y_{ij}^e \bar{L}_L^i \Phi l_R^j + Y_{ij}^u \bar{Q}_L^i \Phi^c u_R^j + Y_{ij}^d \bar{Q}_L^i \Phi d_R^j \xrightarrow{\text{EWSB}} \frac{v}{\sqrt{2}} (Y_{ij}^e \bar{l}_L^i l_R^j + Y_{ij}^u \bar{u}_L^i u_R^j + Y_{ij}^d \bar{d}_L^i d_R^j) \end{aligned}$$

where the Yukawa matrices Y^e , Y^u , Y^d are non-diagonal and fermion masses are proportional to the corresponding eigenvalue. Yukawa couplings for the neutrino fields are not included in \mathcal{L}_y^{F} as in the original formulation of the Standard Model, neutrinos were considered as massless. Ongoing research in neutrino physics however suggests that neutrinos have a non-vanishing mass, which could be implemented in the Standard Model by including right-handed neutrino fields in Tab 2.1.

This brief introduction of the Standard Model can therefore be summarised using Eq. (2.5)-(2.9) by recapitulating the Standard Model Lagrangian, apart from gauge fixing and ghost contributions of the strong sector, as

$$\mathcal{L}_{\text{SM}} = \mathcal{L}_{\text{kin}}^{\text{F}} + \mathcal{L}_{\text{kin}}^{\text{G}} + \mathcal{L}_{\text{kin}}^{\text{H}} - \mathcal{L}_{\text{mass}}^{\text{F}} - V_{\text{Higgs}}.$$

2.5. Flaws of the Standard Model

The previously discussed Standard Model describes the phenomenology at the currently experimentally accessible electroweak scale remarkably well. Yet a few unsatisfactory features of the Standard Model have already been mentioned alongside:

- **Gravitation:** As already stated, the Standard Model is constructed completely omitting gravitation. The Planck scale, at which gravitational effects are no longer negligible, is separated from the electroweak scale by 16 orders of magnitude. This deficit becomes crucial due to the necessity of renormalisation, as Quantum Gravitation requires spin 2 gauge bosons and theories involving such are notoriously non-renormalisable.
- **Arbitrariness:** The Standard Model has 18 free parameters, 25 if nonzero neutrino masses are allowed, which are arbitrary experimental input. By rather aesthetic arguments this is disturbing, as a fundamental theory is considered to answer the question why, instead of how, nature works.

⁴ Φ^c denotes the charge conjugated Higgs doublet field given as: $\Phi^c = i\sigma_2 \Phi^* = ((v + H^*(x))/\sqrt{2}, 0)^T$

- Baryogenesis: The fact that the universe consists of stable particles like protons is the consequence of an imbalance between particles we refer to as matter and their charge conjugated partners. One of the three conditions proposed by A. Sakharov [11] required for the evolution of the universe is the violation of charge (C) and of the combined charge and parity (CP) symmetry. Even though the Standard Model incorporates the violation of C and even the measured simultaneous violation of the CP symmetry can be described by complex phases of the Standard Model parameters, the amount of asymmetry generated by these is not sufficient to explain the known asymmetry of the universe.
- Dark matter: Numerous cosmological observations imply that galaxies are much heavier than estimated by the contribution from the observable massive objects in them. This leads to the conclusion, that there has to be a further kind of massive particles which does not interact by Standard Model interactions.
- Fine-tuning problem: One loop corrections to the Standard Model Higgs boson mass grow quadratically in the cutoff scale Λ which is why a high amount of fine-tuning cancellation of the bare parameters and loop contributions is required to keep the Higgs mass within theoretical bounds when Λ is to be extended far beyond the electroweak scale.

3.1. The Concept of Supersymmetry

While not claiming to be the desired Theory of Everything, Supersymmetry [12–15] offers solutions to most of the previously mentioned flaws. Especially the fine-tuning problem is one of the main motivations for the formulation of Supersymmetry. A complete analysis of radiative corrections of the Standard Model shows, that not only the Higgs mass has a cutoff scale dependence: the fermion and weak boson mass corrections also grow with the cutoff parameter Λ but only logarithmically, while gluons and photons retain zero mass in all orders of perturbation theory. The cutoff sensitivity of masses is thus correlated with the symmetry of the Lagrangian: Gauge symmetries 'protect' photons and gluons from acquiring mass terms and broken symmetries mitigate the cutoff dependence. Therefore, an additional symmetry which affects the Higgs field would soothe the scale dependence of the Higgs mass and the necessity for large fine-tuning can hereby be avoided.

In Supersymmetry this additional symmetry transforms all Standard Model fields into partner fields with identical quantum numbers, except for the spin being shifted by one half of unit. The Supersymmetry generators \mathcal{Q} therefore have to be fermionic operators which, according to the Haag–Lopuszanski–Sohnius theorem [16], are the only possible extension of the symmetry group in four dimensional quantum field theories apart from gauge and Poincaré symmetries. The generators \mathcal{Q} are characterised by their effect on fermionic and bosonic states,

$$\mathcal{Q}|\text{Fermion}\rangle = |\text{Boson}\rangle, \quad \mathcal{Q}|\text{Boson}\rangle = |\text{Fermion}\rangle, \quad (3.1)$$

and by the (anti-)commutation relations

$$\{\mathcal{Q}, \mathcal{Q}\} = \{\bar{\mathcal{Q}}, \bar{\mathcal{Q}}\} = 0 \quad (3.2)$$

$$[\mathcal{Q}, P_\mu] = [\bar{\mathcal{Q}}, P_\mu] = 0 \quad (3.3)$$

$$\{\mathcal{Q}, \bar{\mathcal{Q}}\} = 2\mathcal{P} \quad (3.4)$$

with P^μ being the momentum operator. As a direct consequence of these definitions, the fermionic and bosonic fields connected by Eq. (3.1) can be combined into chiral supermultiplets with equal number of degrees of freedom for both spin states. Additionally, multiplying

Eq. (3.3) with P^μ leads to an equivalent commutation relation with the Poincaré Casimir operator P^2 , yielding

$$[\mathcal{Q}, P^2] = 0 \quad \Rightarrow \quad \mathcal{Q}P^2|n\rangle - P^2\mathcal{Q}|n\rangle = m_n^2|\tilde{n}\rangle - m_{\tilde{n}}^2|\tilde{n}\rangle = 0$$

for an arbitrary state $|n\rangle$ and its superpartner $|\tilde{n}\rangle$. Hence, the superpartners must be of equal mass when Supersymmetry is exact. As no such 'sparticles' were observed at the electroweak scale, Supersymmetry must be a broken symmetry. Soft-breaking terms have to be included in the theory, which produce a mass splitting between the superpartners.

In the most general form of a supersymmetric Lagrangian for a given superfield content, Yukawa-like couplings between sfermions, quarks and leptons occur which violate baryon and lepton number conservation, without contradicting gauge invariance and renormalisability conditions. Such couplings allow rapid proton decay as illustrated in Fig. 3.1, which disagrees with the experimental bound for the proton lifetime being of the order of 10^{34} years. Therefore, an additional \mathbb{Z}_2 symmetry, the multiplicative R -parity, with

$$R|n\rangle = |n\rangle \quad R|\tilde{n}\rangle = -|\tilde{n}\rangle$$

has to be introduced in the theory which allows only terms with positive R -parity in the Lagrangian and thereby rules out the critical couplings. This definition is synonymous to the statement that only couplings with even number of supersymmetric particles are allowed.

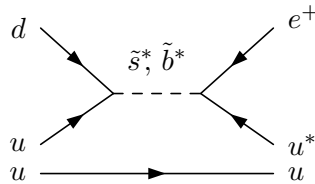


Figure 3.1.: $p^+ \rightarrow e^+\pi^0$ decays via \tilde{s}^* and \tilde{b}^* squark are forbidden by R -parity conservation but not by gauge invariance and renormalisability.

3.2. Solutions provided by Supersymmetry

To finish this short introduction, let us review the flaws stated in section 2.5 regarding the features introduced by Supersymmetry:

- Gravitation and its renormalisation remain issues in supersymmetric theories. Although there are ambitions to incorporate gravitation in supersymmetric string theories in extra dimensions, these attempts, however, are far from achieving phenomenological significance.
- The renormalisation group equations of the Minimal Supersymmetric extension of the Standard Model enable an unification of the three gauge couplings at a scale $\Lambda_{GUT} \sim 10^{16}$ GeV which would allow to summarise all three interactions in a single spontaneously broken symmetry.
- The form of Higgs potential required for spontaneous symmetry breaking does not have to be added ad hoc to the model, as it is the case in the Standard Model. It is generated dynamically by renormalisation group equations.
- Additional complex phases can be included in the Higgs sector of supersymmetric theories which loosen the theoretical bounds for CP violation of the Standard Model and may help to explain baryogenesis.

- Supersymmetry offers Dark Matter candidates, as R -parity conservation implies that a sparticle can not decay into two Standard Model particles. Therefore the lightest sparticle is stable and, when electrically neutral, can interact only weakly.
- As already stated, the fine-tuning problem is likewise solved by Supersymmetry, since the Higgs mass is protected by a broken symmetry and radiative corrections are therefore only logarithmically dependent on the cutoff scale Λ .

3.3. Passing the MSSM

The simplest way to construct a supersymmetric theory is described by the minimal supersymmetric extension of the Standard Model (MSSM) [17–19]. The field content of the MSSM follows from the Standard Model by replacing the Standard Model Higgs doublet field Φ by two Higgs doublets H_u, H_d required to produce mass terms for both up- and down-type fermions, and by promoting the resulting field content to supermultiplets with equivalent bosonic and fermionic degrees of freedom ($H_u \rightarrow \hat{H}_u$ etc.). While being a good starting point for discussions of the phenomenology of Supersymmetry, theoretical analyses reveal insufficiencies of the MSSM. For instance, the tree level mass of the lightest MSSM Higgs boson $m_{h_1}^{\text{MSSM}}$ has to be smaller than the Z boson mass¹,

$$(m_{h_1}^{\text{MSSM}})^2 < m_Z^2 \cos^2 2\beta.$$

Thus, large radiative corrections are required to avoid experimental exclusion limits set by LEP [20]. Additionally, the MSSM superpotential contains terms² proportional to a parameter μ with positive mass dimension,

$$\hat{W}_{\text{MSSM}} \supset \mu \hat{H}_u^T \epsilon \hat{H}_d.$$

This μ -parameter has to be set by hand to the order of the electroweak scale, which is considered as a problem [21]. By this means, some of the solutions proclaimed by Supersymmetry are not satisfactory achieved in the MSSM. These insufficiencies can be avoided by extending the Standard Model in a non-minimal way: The Next-to-Minimal Supersymmetric Extension of the Standard Model (NMSSM) [22–25] is realised by extending the field content of the MSSM by one chiral superfield \hat{S} which is a gauge singlet and therefore does not couple to any Standard Model particles. This minor adjustment loosens the constraints in the Higgs sector, so that the mass of the lightest scalar Higgs boson h_1 gets an additional contribution at tree level

$$(m_{h_1}^{\text{NMSSM}})^2 < m_Z^2 \left[\cos^2 2\beta + \frac{2\lambda^2 \sin^2 2\beta}{g_1^2 + g_2^2} \right].$$

And scenarios of relevance for this thesis, in which the lightest Higgs boson is the pseudoscalar A_1 , become possible. The μ -parameter can then be generated dynamically in the NMSSM from the trilinear coupling

$$\hat{W}_{\text{NMSSM}} \supset \lambda \hat{S} (\hat{H}_u^T \epsilon \hat{H}_d),$$

when the scalar field S acquires a vacuum expectation value $\langle S \rangle = v_s / \sqrt{2}$ in the process of electroweak symmetry breaking,

$$\lambda S (H_u^T \epsilon H_d) \xrightarrow{\text{EWSB}} \underbrace{\frac{\lambda v_s}{\sqrt{2}}}_{\mu_{\text{eff}}} (H_u^T \epsilon H_d),$$

¹The involved angle β is given by the ratio of the vacuum expectation values of $\langle H_u \rangle = v_u / \sqrt{2}$ and $\langle H_d \rangle = v_d / \sqrt{2}$ as $\tan \beta = v_u / v_d$

² ϵ is the SU(2) metric tensor, $\epsilon = \begin{pmatrix} 0 & 1 \\ -1 & 0 \end{pmatrix}$, required to form gauge invariant objects.

where we have defined μ_{eff} as the effective μ parameter. A consequence of this extension is an enlarged Higgs sector of the NMSSM: As shown later on, the neutral Higgs boson spectrum consists of three scalar mass eigenstates (compared to two of the MSSM) and two pseudoscalars (one more than in the MSSM). Likewise, the sector in which the partner particles of the W , Z and of the five neutral Higgs bosons mix to neutral sfermion mass eigenstates, the neutralino sector, is extended by one additional mass eigenstate, compared to the MSSM, to a total of five.

The following chapter introduces the parameters required for the analysis of NMSSM Higgs sector phenomenology and briefly outlines the general strategy of how to derive Feynman rules of a supersymmetric theory with a given superfield content.

3.4. The Lagrangian of the NMSSM

Analogously to the Standard Model, the NMSSM field content can be classified by its transformation behaviour under the gauge group as shown in Tab. 3.1. As already mentioned, the field content can be obtained by including an additional Higgs doublet and a gauge singlet Higgs field to the Standard Model field content and promoting all of these to superfields.

Name/Superfield		Bosonic	Fermionic	SU(3)	SU(2)	U(1)
Chiral	\hat{Q}	$\tilde{Q} = (\tilde{u}_L, \tilde{d}_L)^T$	$Q = (u_L, d_L)^T$	3	2	1/6
	squark/quark	\hat{u}	\tilde{u}_R^*	3	1	-2/3
		\hat{d}	\tilde{d}_R^*	3	1	1/3
	slepton/lepton	\hat{L}	$\tilde{L} = (\tilde{\nu}_{e,L}, \tilde{e}_L)^T$	1	2	-1/2
		\hat{e}	\tilde{e}_R^*	1	1	1
	Higgs/Higgsino	\hat{H}_u	$H_u = (H_u^+, H_u^0)^T$	$\tilde{H}_u = (\tilde{H}_u^+, \tilde{H}_u^0)^T$	1	2
	\hat{H}_d	$H_d = (H_d^0, H_d^-)^T$	$\tilde{H}_d = (\tilde{H}_d^0, \tilde{H}_d^-)^T$	1	2	-1/2
	\hat{S}	S	\tilde{S}	1	1	0
Gauge	gluino/gluon	g	\tilde{g}	8	1	0
	W -boson/wino	W^\pm, W^0	$\tilde{W}^\pm, \tilde{W}^0$	1	3	0
	B -boson/bino	B^0	\tilde{B}^0	1	1	0

Table 3.1.: Gauge and chiral supermultiplets of the NMSSM

Thus, compared to the Standard Model, the particle spectrum of the NMSSM is extended by four neutral (two scalar and two pseudoscalar) and two charged Higgs bosons. Supersymmetry furthermore yields eight additional fermions: these are the five neutralinos $\tilde{\chi}_i^0$ resulting from the mixing of the bino and neutral Higgsino interaction eigenstates, two charginos $\tilde{\chi}_i^\pm$ which are a mixture of the wino and charged Higgsino interaction eigenstates and the gluino \tilde{g} , which is a separate mass eigenstate, since it cannot mix with the other neutral fields as these are colour singlets. For each of the Standard Model fermions l_i , q_i two sleptons $\tilde{L}_{i1}, \tilde{L}_{i2}$ and squarks $\tilde{q}_{i1}, \tilde{q}_{i2}$, respectively, are required in order for the degrees of freedom to be identical among the superpartners.³

The NMSSM superpotential is constructed as an analytic function of up to three chiral superfields invariant under the Standard Model gauge group defined in Eq. (2.4). With minor

³When the neutrinos are considered massless, they each obtain one sneutrino partner particle $\tilde{\nu}_i$ due to the missing degree of freedom.

constraints⁴ this results in

$$\hat{W}_{\text{NMSSM}} = \hat{u}y_u(\hat{Q}^T \epsilon \hat{H}_u) - \hat{d}y_d(\hat{Q}^T \epsilon \hat{H}_d) - \hat{e}y_e(\hat{L}^T \epsilon \hat{H}_d) + \lambda \hat{S}(\hat{H}_u^T \epsilon \hat{H}_d) + \frac{\kappa}{3} \hat{S}^3. \quad (3.5)$$

Here, y_u, y_d, y_e, λ and κ are dimensionless couplings⁵ with the generation indices for the quark and lepton superfields omitted to keep the notation clear. A term cubic in \hat{S} is required, as otherwise the Higgs sector would possess a spontaneously broken Peccei-Quinn (PQ) symmetry, which, according to the Goldstone theorem, would lead to massless axions, for which there is no experimental evidence. Despite the explicit PQ symmetry breaking through the κ -term, the superpotential remains symmetric under discrete \mathbb{Z}_3 transformations. This leads to a topological defect known as the *domain-wall* problem [26], which however can be avoided by modifications far beyond the electroweak scale.

The scalar part of the superpotential reads,

$$W_{\text{NMSSM}} \equiv W = \tilde{u}_R^* y_u (\tilde{Q}^T \epsilon H_u) - \tilde{d}_R^* y_d (\tilde{Q}^T \epsilon H_d) - \tilde{e}_R^* y_e (\tilde{L}^T \epsilon H_d) + \lambda S (H_u^T \epsilon H_d) + \frac{\kappa}{3} S^3. \quad (3.6)$$

The Lagrangian of the unbroken NMSSM, $\mathcal{L}_{\text{susy}}$, can be derived from W using the general strategy described in [25] as,

$$\mathcal{L}_{\text{susy}} = \mathcal{L}_{\text{chiral}} + \mathcal{L}_{\text{gauge}} - \mathcal{L}_{\text{Yukawa}}, \quad \text{with} \quad (3.7)$$

$$\mathcal{L}_{\text{chiral}} = -(\mathcal{D}_\mu \phi_i)^\dagger (\mathcal{D}^\mu \phi_i) - i \psi_i^* \bar{\sigma}^\mu \mathcal{D}_\mu \psi_i + \left| \frac{\partial W}{\partial \phi_i} \right|^2 \quad (3.8)$$

$$\mathcal{L}_{\text{gauge}} = -\frac{1}{4} F_{\mu\nu}^a F^{\mu\nu a} - i \lambda_a^\dagger \bar{\sigma}^\mu \mathcal{D}_\mu \lambda_a + \frac{g_a^2}{2} (\phi_i^* T^a \phi_i) (\phi_j^* T^a \phi_j) \quad (3.9)$$

$$\mathcal{L}_{\text{Yukawa}} = \sqrt{2} g_a ((\phi_i^* T^a \psi_i) \lambda_a + \lambda_a^\dagger (\psi_i^\dagger T^a \phi_i)) + g_a^2 (\phi_i^* T^a \phi_i) (\phi_j^* T^a \phi_j), \quad (3.10)$$

where ϕ_i are the scalar components of chiral superfields, ψ_i the associated Weyl fermions, λ^a the gauge boson superpartners and T^a, g_a is a synoptic notation for the Standard Model gauge group generators and couplings.

Soft-breaking terms have to be included separately to generate the required mass splitting between the superpartners. The breaking terms are introduced in the most general way [27] in terms of the bosonic (fermionic) components of the chiral (gauge) superfields,

$$\begin{aligned} \mathcal{L}_{\text{soft}} = & m_{\tilde{Q}_L}^2 \tilde{Q}^\dagger \tilde{Q} + m_{\tilde{L}_L}^2 \tilde{L}^\dagger \tilde{L} + m_{\tilde{u}_R}^2 |\tilde{u}_R|^2 + m_{\tilde{d}_R}^2 |\tilde{d}_R|^2 + m_{\tilde{e}_R}^2 |\tilde{e}_R|^2 + m_{H_u}^2 H_u^\dagger H_u + m_{H_d}^2 H_d^\dagger H_d + \\ & + m_S^2 |S|^2 + \left(y_u A_{y_u} \tilde{u}_R^* (\tilde{Q}^T \epsilon H_u) - y_d A_{y_d} \tilde{d}_R^* (\tilde{Q}^T \epsilon H_d) - y_e A_{y_e} \tilde{e}_R^* (\tilde{L}^T \epsilon H_d) + c.c. \right) + \\ & + \left(\frac{M_1}{2} \tilde{B}^0 \tilde{B}^0 + \frac{M_2}{2} \tilde{W}_i \tilde{W}^i + \frac{M_3}{2} \tilde{g} \tilde{g} + \lambda A_\lambda S (H_u^T \epsilon H_d) + \frac{\kappa A_\kappa}{3} S^3 + c.c. \right), \end{aligned} \quad (3.11)$$

where the squark and slepton sectors are again abbreviated by including only their first generation. Thus, in the most general case $\mathcal{L}_{\text{soft}}$ introduces 21 soft breaking masses m_i^2 and 11 trilinear couplings A_i via which soft Supersymmetry breaking is achieved. Since the circumstances under which Supersymmetry is broken are nebulous and out of reach of experimental analysis, the majority of parameters is set to a fixed scale in constrained versions of the NMSSM. The complete NMSSM Lagrangian can thus be formulated as

$$\mathcal{L}_{\text{NMSSM}} = \mathcal{L}_{\text{chiral}} + \mathcal{L}_{\text{gauge}} - \mathcal{L}_{\text{Yukawa}} - \mathcal{L}_{\text{soft}}. \quad (3.12)$$

⁴Terms analogous to the MSSM μ -term and quadratic in \hat{S} could be included in general, they are omitted to keep the superpotential free of dimensionful parameters.

⁵The parameters y_u, y_d and y_e replace the Standard Model Yukawa matrices, which are considered to be diagonal for simplicity, i.e. generation mixing is neglected.

Together with the Higgs field vacuum expectation values v_d , v_u , v_s , and the Standard Model gauge couplings g_1 , g_2 , the parameters of interest for NMSSM Higgs sector phenomenology can be summarised as

$$g_1, g_2, v_d, v_u, v_s, \lambda, \kappa, A_\lambda, A_\kappa, m_{H_d}^2, m_{H_u}^2, m_S^2. \quad (3.13)$$

In the CP conserving case, these 12 quantities are all real parameters which require renormalisation in higher order calculations. Before we determine the renormalisation conditions, let us examine the NMSSM Higgs potential in detail.

3.5. The Scalar NMSSM Higgs Potential

The Higgs sector offers a good starting point for a detailed discussion of how Feynman rules can be derived from the superpotential. It involves mixing of interaction fields, which is ubiquitous in supersymmetric models and the occurring quantities are of the essence for the calculations performed in this thesis, as well as suitable for the definition of the renormalisation conditions required for the determination of the counterterms.

The scalar Higgs potential V_H can be derived from the scalar superpotential Eq. (3.6) as

$$V_H = \mathcal{L}_{\text{soft}}|_{\text{Higgs}} + V_F|_{\text{Higgs}} + V_D|_{\text{Higgs}}. \quad (3.14)$$

The indices meaning, that only terms which depend on Higgs fields are taken into account. With $\mathcal{L}_{\text{soft}}$ defined in Eq. (3.11) and the V_D and V_F terms defined as

$$V_D = \frac{1}{2} \sum_{i,j} g_a^2 (\phi_i^\dagger T^a \phi_i) (\phi_j^\dagger T^a \phi_j) \quad (3.15)$$

$$V_F = \sum_i \left| \frac{\partial W}{\partial \phi_i} \right|^2. \quad (3.16)$$

The scalar Higgs potential reads

$$\begin{aligned} V_H = & m_{H_u}^2 H_u^\dagger H_u + m_{H_d}^2 H_d^\dagger H_d + m_S^2 |S|^2 + (\lambda A_\lambda (H_u^T \epsilon H_d) S + \frac{\kappa A_\kappa}{3} S^3 + c.c.) + \\ & + \lambda^2 |S|^2 (H_u^\dagger H_u + H_d^\dagger H_d) + |\lambda (H_u^T \epsilon H_d) + \kappa S^2|^2 + \\ & + \frac{1}{2} g_2^2 |H_u^\dagger H_d|^2 + \frac{1}{8} (g_1^2 + g_2^2) (H_u^\dagger H_u + H_d^\dagger H_d). \end{aligned} \quad (3.17)$$

Parametrising the complex doublets H_u , H_d and the singlet S as

$$H_d = \begin{pmatrix} \frac{1}{\sqrt{2}}(v_d + h_d + i a_d) \\ H_d^- \end{pmatrix}, \quad H_u = \begin{pmatrix} H_u^+ \\ \frac{1}{\sqrt{2}}(v_u + h_u + i a_u) \end{pmatrix}, \quad S = \frac{1}{\sqrt{2}}(v_s + h_s + i a_s)$$

the potential can be decomposed into products of up to four real scalar fields h_u , h_d , h_s , a_u , a_d , a_s and complex scalar fields H_u^+ , H_d^- , from which Feynman rules can be derived in a straightforward way. However, this involves cumbersome long terms, which is why some simplifications should be done beforehand.

The number of tree level parameters can be decimated by exploiting the stationarity condition of the potential at its vacuum expectation value, the so called tadpole conditions:

$$\begin{aligned} t_{h_d} = \left\langle \frac{\partial V_H}{\partial h_d} \right\rangle &= v_d m_{H_d}^2 - \frac{\lambda A_\lambda v_u v_s}{\sqrt{2}} + \frac{g_1^2 + g_2^2}{8} v_d (v_d^2 - v_u^2) + \frac{\lambda^2 v_d}{2} (v_u^2 + v_s^2) - \frac{\lambda \kappa v_u v_s^2}{2} = 0 \\ t_{h_s} = \left\langle \frac{\partial V_H}{\partial h_s} \right\rangle &= v_s m_S^2 - \frac{\lambda A_\lambda v_d v_u}{\sqrt{2}} + \frac{\kappa A_\kappa v_s^2}{\sqrt{2}} + \frac{\lambda^2}{2} v_s (v_d^2 + v_u^2) + \kappa^2 v_s^3 - \lambda \kappa v_d v_u v_s = 0 \\ t_{h_u} = \left\langle \frac{\partial V_H}{\partial h_u} \right\rangle &= v_u m_{H_u}^2 - \frac{\lambda A_\lambda v_d v_s}{\sqrt{2}} + \frac{g_1^2 + g_2^2}{8} v_u (v_u^2 - v_d^2) + \frac{\lambda^2 v_u}{2} (v_d^2 + v_s^2) - \frac{\lambda \kappa v_d v_s^2}{2} = 0. \end{aligned} \quad (3.18)$$

As the mass matrices are symmetric, the missing elements follow from the second column with the relation $m_{ij} = m_{ji}$. Before \mathcal{M}_1 is diagonalised, the Goldstone field required to generate the Z -boson mass can be isolated by a rotation in the pseudoscalar sector

$$\phi \rightarrow \phi' = R_T \phi = (h_d, h_u, h_s, G, a, a_s)^T, \quad (3.25)$$

$$R_T = \begin{pmatrix} \mathbb{I}_{3 \times 3} & 0_{3 \times 3} \\ 0_{3 \times 3} & \begin{pmatrix} c_{\beta_B} & -s_{\beta_B} & 0 \\ s_{\beta_B} & c_{\beta_B} & 0 \\ 0 & 0 & 1 \end{pmatrix} \end{pmatrix}. \quad (3.26)$$

The rotation angle β_B coincides with the angle β introduced in Eq. (3.19) at tree level, but attention has to be paid when performing higher order calculations, as by convention mixing matrix elements do not require renormalisation, whereas t_β being the ratio of the vacuum expectation values is a model parameter and therefore has to be renormalised. The transformation Eq. (3.25) thus transforms the lower right entries of \mathcal{M}_1 and the resulting mass matrix \mathcal{M}'_1 can be diagonalised via the rotation matrix R_H ,

$$\phi'^T \mathcal{M}'_1 \phi' = \phi'^T R_H^T R_H \mathcal{M}'_1 R_H^T R_H \phi' = \mathbf{h}^T \mathcal{M}_h \mathbf{h} = m_i^2 \mathbf{h}_i^2. \quad (3.27)$$

The two rotations R_T, R_H can be combined to a single transformation connecting the interaction field basis ϕ and mass field basis \mathbf{h} ,

$$\mathcal{R} = R_H R_T \quad (3.28)$$

$$\mathbf{h} = \mathcal{R} \phi = (h_1, h_2, h_3, A_1, A_2, G) \quad (3.29)$$

$$\mathcal{R} \mathcal{M}_1 \mathcal{R}^T = \text{diag}(m_{h_1}^2, m_{h_2}^2, m_{h_3}^2, m_{A_1}^2, m_{A_2}^2, 0). \quad (3.30)$$

The basis \mathbf{h} can be chosen such, that the eigenvalues of the scalar and the pseudoscalar block of \mathcal{M}_1 in Eq. (3.30) are in ascending order, with the Goldstone mode rotated out and usually omitted entirely.

3.5.2. Charged Higgs Boson Mass Matrix

The charged Higgs mass matrix \mathcal{M}_2 can be treated analogously. With respect to the basis χ it is found to be,

$$\mathcal{M}_2 = \left(\frac{\lambda v_s}{2} (\kappa v_s + \sqrt{2} A_\lambda) + \frac{s_{2\beta} v^2}{8} (g_2^2 - 2\lambda^2) \right) \begin{pmatrix} t_\beta & 1 \\ 1 & t_\beta^{-1} \end{pmatrix}. \quad (3.31)$$

Just like in the neutral sector, the Goldstone mode required to generate the W -boson mass can be isolated by a rotation

$$\chi \rightarrow \mathbf{H} = \mathcal{R}^\pm \chi = (G^\pm, H^\pm)^T \quad (3.32)$$

$$\mathcal{R}^\pm = \begin{pmatrix} c_{\beta_B} & -s_{\beta_B} \\ s_{\beta_B} & c_{\beta_B} \end{pmatrix}. \quad (3.33)$$

Using the Standard Model definition $m_W = g_2 v / 2$, the tree level mass squared of the charged Higgs bosons $m_{H^\pm}^2$ reads

$$m_{H^\pm}^2 = m_W^2 - \frac{\lambda^2 v^2}{2} + \frac{\lambda v_s}{s_{2\beta}} (\kappa v_s + \sqrt{2} A_\lambda). \quad (3.34)$$

It is convenient to replace A_λ with $m_{H^\pm}^2$ as model parameter since, as a mass parameter, it can be renormalised on-shell. Using the orthogonality relation of the rotation matrices \mathcal{R} , \mathcal{R}^\pm , the Higgs potential given in Eq. (3.20) can be rewritten in terms of the mass eigenstates as

$$\begin{aligned}
V_H = & \frac{1}{2} \mathcal{M}_1^{ij} \mathcal{R}_{\alpha i} \mathcal{R}_{\beta j} \mathbf{h}_\alpha \mathbf{h}_\beta + \frac{1}{2} \mathcal{M}_2^{ij} \mathcal{R}_{\alpha i}^\pm \mathcal{R}_{\beta j}^\pm \mathbf{H}_\alpha \mathbf{H}_\beta + \\
& + \Gamma_1^{ijk} \mathcal{R}_{\alpha i} \mathcal{R}_{\beta j} \mathcal{R}_{\gamma k} \mathbf{h}_\alpha \mathbf{h}_\beta \mathbf{h}_\gamma + \Gamma_2^{ijk} \mathcal{R}_{\alpha i} \mathcal{R}_{\beta j}^\pm \mathcal{R}_{\gamma k}^\pm \mathbf{h}_\alpha \mathbf{H}_\beta \mathbf{H}_\gamma + \\
& + \Delta_1^{ijkl} \mathcal{R}_{\alpha i} \mathcal{R}_{\beta j} \mathcal{R}_{\gamma k} \mathcal{R}_{\delta l} \mathbf{h}_\alpha \mathbf{h}_\beta \mathbf{h}_\gamma \mathbf{h}_\delta + \\
& + \Delta_2^{ijkl} \mathcal{R}_{\alpha i} \mathcal{R}_{\beta j} \mathcal{R}_{\gamma k}^\pm \mathcal{R}_{\delta l}^\pm \mathbf{h}_\alpha \mathbf{h}_\beta \mathbf{H}_\gamma \mathbf{H}_\delta + \\
& + \Delta_3^{ijkl} \mathcal{R}_{\alpha i}^\pm \mathcal{R}_{\beta j}^\pm \mathcal{R}_{\gamma k}^\pm \mathcal{R}_{\delta l}^\pm \mathbf{H}_\alpha \mathbf{H}_\beta \mathbf{H}_\gamma \mathbf{H}_\delta.
\end{aligned}$$

Thus, the Feynman rules for the trilinear and quartic Higgs boson couplings can be read off as i times the coefficient of the mass fields

$$\begin{aligned}
\mathbf{g}_{\alpha\beta\gamma}^{3\mathbf{h}} &= i \Gamma_1^{ijk} \mathcal{R}_{\alpha i} \mathcal{R}_{\beta j} \mathcal{R}_{\gamma k} \\
\mathbf{g}_{\alpha\beta\gamma}^{\mathbf{h}2\mathbf{H}} &= i \Gamma_2^{ijk} \mathcal{R}_{\alpha i} \mathcal{R}_{\beta j}^\pm \mathcal{R}_{\gamma k}^\pm \\
\mathbf{g}_{\alpha\beta\gamma\delta}^{4\mathbf{h}} &= i \Delta_1^{ijkl} \mathcal{R}_{\alpha i} \mathcal{R}_{\beta j} \mathcal{R}_{\gamma k} \mathcal{R}_{\delta l} \\
\mathbf{g}_{\alpha\beta\gamma\delta}^{2\mathbf{h}2\mathbf{H}} &= i \Delta_2^{ijkl} \mathcal{R}_{\alpha i} \mathcal{R}_{\beta j} \mathcal{R}_{\gamma k}^\pm \mathcal{R}_{\delta l}^\pm \\
\mathbf{g}_{\alpha\beta\gamma\delta}^{4\mathbf{H}} &= i \Delta_3^{ijkl} \mathcal{R}_{\alpha i}^\pm \mathcal{R}_{\beta j}^\pm \mathcal{R}_{\gamma k}^\pm \mathcal{R}_{\delta l}^\pm.
\end{aligned} \tag{3.35}$$

Since the trilinear neutral Higgs coupling $\mathbf{g}_{\alpha\beta\gamma}^{3\mathbf{h}}$ is of central importance for this thesis, its explicit form is included in App. A. The other sectors of the NMSSM can be treated in a similar way, implying rotation matrices required to determine the Feynman rules, which then can be expressed in terms of the parameters discussed in this chapter.

Introduction to Renormalisation

The key feature of extensions of the Standard Model such as the NMSSM is that if the model parameters are chosen correctly, one can not only try to reconstruct known experimental results of elementary particle physics but also predict so far unobserved phenomena. In order to validate the parameter choice, respectively the model itself, one has to calculate quantities related to observables. From the theoreticians' point of view these calculations involve the determination of the amplitudes \mathcal{M}_{fi} , which describe the probability of a transition from the initial state $|i\rangle$ to a certain final state $|f\rangle$ in a perturbative manner. The square of the absolute value of \mathcal{M}_{fi} weighted with appropriate kinematical terms, corresponds to experimental observables such as the decay width and the cross section.

The advantage of the Feynman rules technique introduced in [28] is, that one can derive the amplitude of any process in an intuitive diagrammatic approach:

- Draw propagators of the incoming and outgoing particles and connect them in every imaginable way¹ allowed by the Feynman rules of the model.
- Replace the propagator lines and vertices in each diagram by their mathematical equivalents².
- Diagrams with enclosed internal lines (so-called loops) depend on the loop-momentum over which one has to integrate.
- The full amplitude is the sum of all contributing diagrams.

Depending on how blooming the imagination is, the reader might have noticed, that the number of possibilities to connect the initial and final states is sheer endless. This fact is not further disturbing when one realises, that in a perturbative theory every vertex is proportional to a small coupling constant. Therefore contributions from diagrams with additional vertices (which are closely related to diagrams with a higher number of loops) are numerically suppressed and formally count to higher order corrections of the perturbation expansion.

At this point, one can question the necessity of loop contributions, since they seem to be mere corrections. Nevertheless, these have vast phenomenological consequences in many cases, as

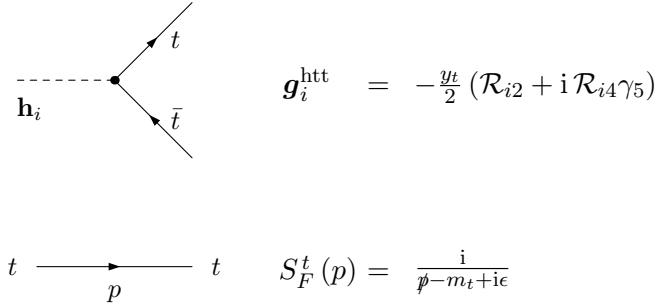
¹It is sufficient to take only fully connected diagrams into account.

²Due to their non-commuting nature, fermionic terms must be multiplied in strict order reverse to the fermion flow direction. Additionally, each enclosed fermion line produces an overall factor of (-1).

they can enable processes not present at tree level (to name a prominent example just consider Higgs production in gluon fusion, the main production channel for the Standard Model Higgs at the LHC), or modify parameters substantially (cf. the mass of the lightest MSSM Higgs boson as discussed in the previous chapter), so that good accordance with the experimental precision tests is only achievable, when higher order contributions are included.

4.1. Of Loops and Infinities

A further flaw of these calculations seems to arise from diagrams involving loops, because the loop-momentum integration can lead to divergent amplitudes. Let us investigate this by looking at the example of the top quark one-loop correction to the NMSSM Higgs coupling between the lightest scalar Higgs boson h_1 and two light pseudoscalar Higgs bosons A_1 . Following the conventions of the previous chapter (where $\mathbf{h}_4 = A_1$ etc.), the relevant Feynman rules for this calculation can be found as



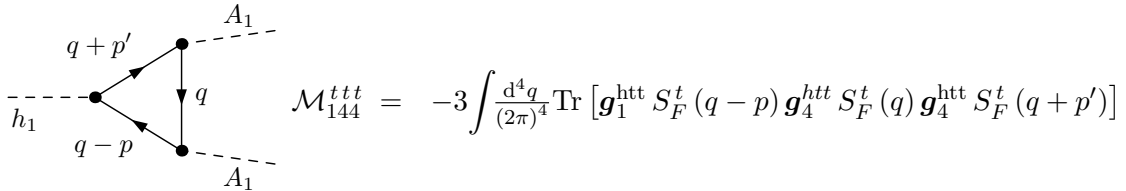
The figure shows two Feynman rules. The first is a vertex where a dashed line labeled \mathbf{h}_i enters from the left and splits into two solid lines labeled t and \bar{t} exiting to the right. The second is a propagator where a solid line labeled t enters from the left and exits to the right, with momentum p indicated below the line.

$$\mathbf{h}_i \quad \begin{array}{l} \nearrow t \\ \searrow \bar{t} \end{array} \quad \mathbf{g}_i^{\text{htt}} = -\frac{yt}{2} (\mathcal{R}_{i2} + i\mathcal{R}_{i4}\gamma_5)$$

$$t \xrightarrow{p} t \quad S_F^t(p) = \frac{i}{\not{p} - m_t + i\epsilon}$$

Figure 4.1.: Feynman rules for the NMSSM Higgs-boson-top-quark vertex and the top propagator

where γ_5 is the product of the four Dirac matrices, $\gamma_5 = i\gamma_0\gamma_1\gamma_2\gamma_3$, and the non-trivial colour and spinor index structure of the top quark is omitted for simplicity. Their effect is taken into account by multiplying the resulting amplitude with a factor of (-3) and by taking the trace over the gamma matrices. Also notice that in the CP-conserving case either \mathcal{R}_{i4} or \mathcal{R}_{i2} equals zero, depending on whether the involved Higgs is scalar (CP even) or pseudoscalar (CP odd). Because the diagram in Fig. 4.2 contains 3 vertices, we can eliminate 3 of the 6 propagator momenta using momentum conservation at the three vertices. The remaining 3 are chosen to be combinations of the loop momentum³ q and the momenta of the final states p, p' .



The figure shows a loop diagram and its corresponding amplitude. The diagram has an incoming dashed line labeled h_1 from the left. It splits into two solid lines labeled t and \bar{t} . The t line goes up and right to a vertex, then loops back down and left to another vertex. The \bar{t} line goes down and right to a vertex, then loops back up and left to the same vertex. From the top vertex, a dashed line labeled A_1 goes up and right. From the bottom vertex, a dashed line labeled A_1 goes down and right. Momenta are labeled: $q+p'$ for the top vertex, $q-p$ for the bottom vertex, and q for the loop. The amplitude is given by:

$$\mathcal{M}_{144}^{ttt} = -3 \int \frac{d^4q}{(2\pi)^4} \text{Tr} [\mathbf{g}_1^{\text{htt}} S_F^t(q-p) \mathbf{g}_4^{\text{htt}} S_F^t(q) \mathbf{g}_4^{\text{htt}} S_F^t(q+p')]$$

Figure 4.2.: Example process for divergent loop diagrams and its amplitude in terms of Fig. 4.1

³By convention, the momentum of initial (final) state fields is chosen to point towards (out of) the vertex. The momentum of fermionic fields points in the fermion flow direction.

Using the Feynman rules given above, the amplitude stated in Fig. 4.2 can be written as

$$\begin{aligned} \mathcal{M}_{144}^{ttt} &= -3 \int \frac{d^4 q}{(2\pi)^4} \text{Tr} \left[\left(-\frac{y_t}{2} \mathcal{R}_{12} \right) \frac{i}{\not{q} - \not{p} - m_t + i\epsilon} \left(-\frac{iy_t}{2} \mathcal{R}_{44} \gamma_5 \right) \frac{i}{\not{q} - m_t + i\epsilon} \left(-\frac{iy_t}{2} \mathcal{R}_{44} \gamma_5 \right) \frac{i}{\not{q} + \not{p}' - m_t + i\epsilon} \right] \\ &= -3i \mathcal{R}_{12} \mathcal{R}_{44}^2 \left(\frac{y_t}{2} \right)^3 \int \frac{d^4 q}{(2\pi)^4} \text{Tr} \left[\frac{\not{q} - \not{p} + m_t}{(q-p)^2 - m_t^2 + i\epsilon} \gamma_5 \frac{\not{q} + m_t}{q^2 - m_t^2 + i\epsilon} \gamma_5 \frac{\not{q} + \not{p}' + m_t}{(q+p')^2 - m_t^2 + i\epsilon} \right]. \end{aligned}$$

Rewriting the propagators, the denominators become scalar quantities and can therefore be factorised out of the trace, the remaining nominator trace term can then be evaluated with the help of known identities for Dirac matrices,

$$\begin{aligned} \text{Tr} \left[(\not{q} - \not{p} + m_t) \gamma_5 (\not{q} + m_t) \gamma_5 (\not{q} + \not{p}' + m_t) \right] &= -4 m_t (q^2 - m_t^2 + pp') \\ \rightarrow \mathcal{M}_{144}^{ttt} &= 12i \mathcal{R}_{12} \mathcal{R}_{44}^2 \left(\frac{y_t}{2} \right)^3 m_t \int \frac{d^4 q}{(2\pi)^4} \frac{q^2 - m_t^2 + pp'}{((q-p)^2 - m_t^2 + i\epsilon)(q^2 - m_t^2 + i\epsilon)((q+p')^2 - m_t^2 + i\epsilon)}. \end{aligned} \quad (4.1)$$

Next we apply the so-called Feynman trick to bring the integrand I of Eq. (4.1) into a neater form

$$\begin{aligned} I &= I_1 + I_2 \\ &= \frac{1}{((q-p)^2 - m_t^2 + i\epsilon)((q+p')^2 - m_t^2 + i\epsilon)} + \frac{pp'}{((q-p)^2 - m_t^2 + i\epsilon)(q^2 - m_t^2 + i\epsilon)((q+p')^2 - m_t^2 + i\epsilon)} \\ &= \int_0^1 dx \frac{1}{(q_1^2 - m_1 + i\epsilon)^2} + \int_0^1 dx \int_0^{1-x} dy \frac{pp'}{(q_2^2 - m_2 + i\epsilon)^3}, \end{aligned} \quad (4.2)$$

where the following substitutions have been made:

$$\begin{aligned} q_1 &= q - p + x(p + p') \\ m_1 &= x(x-1)(p + p')^2 + m_t^2 \\ q_2 &= q - xp + yp' \\ m_2 &= x(x-1)p^2 + y(y-1)p'^2 + m_t^2 - 2xypp'. \end{aligned} \quad (4.3)$$

The last step before the integral can be evaluated involves transforming the Minkowski metric of the integral to Euclidean space by a Wick rotation. For a detailed discussion on how this is performed, see [29]. Ultimately, since I depends solely on the squares of momenta, this Euclidean integral is solvable in 4 dimensional polar coordinates.

$$\int \frac{d^4 q_1}{(2\pi)^4} I_1 = \lim_{a \rightarrow 0} i \int_0^1 dx \int_0^1 \frac{dq_1}{8\pi^2} \frac{q_1^3}{(q_1^2 + m_1 - i\epsilon)^2} \rightarrow \text{divergent} \quad (4.4)$$

$$\int \frac{d^4 q_2}{(2\pi)^4} I_2 = \lim_{a \rightarrow 0} i \int_0^1 dx \int_0^{1-x} dy \int_0^{1/a} \frac{dq_2}{8\pi^2} \frac{q_2^3}{(q_2^2 + m_2 - i\epsilon)^3} \rightarrow \text{finite} \quad (4.5)$$

The integral over I_1 diverges logarithmically as the cutoff parameter $1/a$ is sent to infinity. Such a behaviour is referred to as ultraviolet (UV) divergence.

4.2. The Concept of Renormalisation

Divergent results similar to that of Eq. (4.4), along with infrared (IR) divergences occurring in loop diagrams containing massless particles⁴, have puzzled physicists since the early 1930s.

⁴Since Higgs bosons couple exclusively to massive particles, we do not have to be concerned about IR divergences in the scope of this thesis.

Fortunately, a solution to this problem was found through renormalisation, suggesting that the ‘bare’ parameters of a theory are not equal to the ones measured in experiments. In fact, the former are infinite and it is due to a ‘screening effect’ of these UV divergent higher order processes, that the parameters adopt their experimentally measured finite values. This concept of subtracting infinities might sound disturbing and has led to much scepticism among physicists throughout the decades - even the creators of quantum field theory⁵ and quantum electrodynamics⁶ were not satisfied with the explanations the renormalisation procedure offers. Nevertheless, the reservations towards this mathematically questionable approach have settled. From today’s point of view, the Standard Model is considered to be an effective low energy limits of an eventual ‘theory of everything’ and, as has been shown by ’t Hooft and Veltman, it can be renormalised in a self-consistent way, yielding results in remarkable agreement with experimental data.

4.3. General Renormalisation Procedure

Let us take a closer look at how finite next-to-leading order results can be obtained using renormalisation. The first step is to define a consistent treatment of divergent contributions from loop integrals and counterterms. For this purpose, an additional parameter, the regulator λ , is introduced in the theory in such a way, that all divergent integrals become finite, except for the limit $\lambda = \lambda_0$ for which the original divergent theory is restored. Renormalisation is successfully achieved, when the λ dependence of the loop and counterterm contributions cancel each other.

4.3.1. Methods of Regularisation

There are several ways to regularise integrals, but some are more suitable because of the symmetries of the Lagrangian. For instance, we have already encountered the most obvious regularisation method in Eq. (4.4) where the regulator is the cutoff momentum $\lambda = 1/a$ and the original theory is restored in the limit $\lambda \rightarrow \infty$. While the calculation is vivid for qualitative discussion, one would face difficulties proving Ward identities, which require translational invariance in momentum space.

A method respecting the symmetries of the Standard Model was introduced in 1972 by ’t Hooft and Veltman [32] called Dimensional Regularisation. The regulator in this case is the dimensionality of spacetime $\lambda = D$, often rearranged to a more convenient form $D = 4 - 2\varepsilon$ so that the 4 dimensional threshold is restored for $\varepsilon \rightarrow 0$. Since the mass dimension of the differential dx equals -1 in natural units, the Lagrangian has to be D dimensional for the action S to remain scalar. Straightforward dimensional analysis then implies that originally dimensionless parameters would depend on D . For this reason an arbitrary fixed mass scale μ has to be defined to absorb the dimensional dependence of dimensionless couplings. Therefore, using the rules of dimensional regularisation, we replace

$$\int \frac{d^4q}{(2\pi)^4} \rightarrow \mu^{4-D} \int \frac{d^Dq}{(2\pi)^D}.$$

⁵“I must say that I am very dissatisfied with the situation, because this so-called ‘good theory’ does involve neglecting infinities which appear in its equations, neglecting them in an arbitrary way. This is just not sensible mathematics. Sensible mathematics involves neglecting a quantity when it is small - not neglecting it just because it is infinitely great and you do not want it!” – P. A. M. Dirac, referring to QED [30].

⁶“But no matter how clever the word, it is still what I would call a dippy process! Having to resort to such hocus-pocus has prevented us from proving that the theory of quantum electrodynamics is mathematically self-consistent. It’s surprising that the theory still hasn’t been proved self-consistent one way or the other by now; I suspect that renormalisation is not mathematically legitimate.” – R. P. Feynman, referring to renormalisation [31].

The example discussed in Sec. 4.1 yields

$$B_0 := \mu^{4-D} \int \frac{d^D q_1}{(2\pi)^D} I_1 = \Omega_D \frac{(2\pi\mu)^{4-D}}{(2\pi)^4} \int_0^1 dx \int_0^\infty dq_1 \frac{q_1^{D-1}}{(q_1^2 + m_1 - i\epsilon)^2},$$

with Ω_D being the surface of the $D-1$ dimensional unit sphere,

$$\Omega_D = \frac{2\pi^{D/2}}{\Gamma(D/2)}.$$

The substitution $q_1^2 = y(m_1 - i\epsilon)$ leads to an Euler integral of the first kind:

$$\begin{aligned} B_0 &= \frac{(2\pi\mu^2)^{\frac{4-D}{2}}}{8\pi^2 \Gamma(\frac{D}{2})} \int_0^1 dx (m_1 - i\epsilon)^{\frac{D-4}{2}} \underbrace{\int_0^\infty dy y^{\frac{D-2}{2}} (y+1)^{-2}}_{B(\frac{D}{2}, \frac{4-D}{2})} \\ B_0 &= \frac{\Gamma(\frac{4-D}{2})}{8\pi^2} \int_0^1 dx \left[\frac{m_1 - i\epsilon}{2\pi\mu^2} \right]^{\frac{D-4}{2}} = \frac{\Gamma(\varepsilon)}{8\pi^2} \int_0^1 dx \left[\frac{m_1 - i\epsilon}{2\pi\mu^2} \right]^{-\varepsilon}. \end{aligned}$$

Resubstituting m_1 according to Eq. (4.3) and taking the limit $\varepsilon \rightarrow 0$ results in

$$B_0 = \frac{1}{8\pi^2} \underbrace{\left[\frac{1}{\varepsilon} - \gamma_E + \log 4\pi \right]}_{=: \Delta} - \frac{1}{8\pi^2} \int_0^1 dx \log \left[\frac{x(x-1)(p+p')^2 + m_t^2 - i\epsilon}{\mu^2/2} \right] + \mathcal{O}(\varepsilon). \quad (4.6)$$

Even though the remaining integral in Eq. (4.6) is too elaborate to be solved analytically, it converges so that we have managed to regularise the divergence as a $1/\varepsilon$ pole⁷. Following this procedure, one can reduce arbitrary one-loop amplitudes to sums of scalar Passarino-Veltman integrals defined for example in the `LoopTools` manual [34].

Dimensional Regularisation is not a suitable regularisation method for supersymmetric theories, as the degrees of freedom of the bosonic and fermionic components of a superfield do not match in arbitrary dimensions and additional supersymmetry restoring terms have to be included in order to preserve unitarity. This is why a technique called Dimensional Reduction [33], has been developed. Unlike in Dimensional Regularisation, only the spacetime and momentum dimensionality is analytically continued into D dimensions, while fields and the γ -matrices are kept four dimensional, by which discrepancies in the degrees of freedom are avoided. In one loop calculations the Dimensional Reduction procedure has been shown [34] to be equivalent to the method of Constrained Differential Regularisation [35], which is implemented in the programs used for computation in this thesis discussed in Chapter 5.

4.3.2. Counterterm Formalism

As mentioned previously, in next-to-leading order calculations the bare parameters ξ_0 of a theory must be replaced by sums of finite renormalised quantities ξ_R and divergent counterterms $\delta\xi$,

$$\xi_0 \rightarrow \xi_R + \delta\xi. \quad (4.7)$$

⁷Since the pole is always accompanied by the Euler–Mascheroni constant γ_E and $\log 4\pi$, these are frequently abbreviated with Δ as stated in Eq. (4.6).

Higher order corrections not only shift the position of a propagator's pole in the complex plane but also its residue, thus it is necessary to renormalise the fields as well, hence

$$\phi_0 \rightarrow \sqrt{Z_\phi} \phi_R = \sqrt{1 + \delta Z_\phi} \phi_R. \quad (4.8)$$

Applying these substitutions, the Lagrangian can be split into a part the structure of which is identical to the tree level Lagrangian, except for the bare parameters being replaced by the physical quantities, and a counterterm part, which yields additional Feynman rules.

$$\mathcal{L} = \mathcal{L}_P + \delta\mathcal{L}. \quad (4.9)$$

4.3.3. Renormalisation Conditions

The counterterms can be determined by demanding that the propagators of the renormalised fields have the same pole structure (position and residue) as the corresponding free field propagators.

The renormalised propagator $\Delta_s(q)$ of a scalar field of mass m_R is given as a sum of chains of one-particle-irreducible subgraphs $\hat{\Sigma}_s(q^2)$ connected with corrected propagators

$$\begin{aligned} \Delta_s(q) &= i \sum_{n=0}^{\infty} [q^2 - m_R^2 + i\epsilon]^{-1} \left(\hat{\Sigma}_s(q^2) [q^2 - m_R^2 + i\epsilon]^{-1} \right)^n \\ &= i \left[q^2 - m_R^2 - \hat{\Sigma}_s(q^2) + i\epsilon \right]^{-1}. \end{aligned} \quad (4.10)$$

For the renormalised propagator $\Delta_s(q)$ to have the same pole structure as the bare one, the conditions

$$\text{Re } \hat{\Sigma}_s(m_R^2) = 0, \quad 0 = \text{Re} \left. \frac{\partial \hat{\Sigma}_s(q^2)}{\partial q^2} \right|_{q^2=m_R^2} \quad (4.11)$$

must be fulfilled. Since $\hat{\Sigma}_s^{\text{nl0}}(q^2)$ is the sum of the $\delta\mathcal{L}$ counterterm contributions to the propagator (i.e. all terms quadratic in the field) and the one-loop self-energies,

$$\hat{\Sigma}_s^{\text{nl0}}(q^2) = \Sigma_s^{\text{ct}}(q^2) + \Sigma_s^{\text{nl0}}(q^2), \quad (4.12)$$

the counterterms δm_p^2 and δZ_ϕ can be expressed in terms of one-loop propagator corrections. Similar conditions can be derived for corrections to the gauge boson propagators $\Delta_{\mu\nu}^V$ where the one-particle-irreducible subgraphs can be decomposed into Lorentz-covariant longitudinal and transversal components, leading to the corrected inverse propagators in the 't Hooft-Feynman gauge to be of the form:

$$(\Delta_{\mu\nu}^W)^{-1} = -ig_{\mu\nu}(q^2 - m_W^2) - i \left(g_{\mu\nu} - \frac{q_\mu q_\nu}{q^2} \right) \hat{\Sigma}_T^W(q^2) - i \frac{q_\mu q_\nu}{q^2} \hat{\Sigma}_L^W(q^2) \quad (4.13)$$

for the W boson and

$$(\Delta_{\mu\nu}^{ab})^{-1} = -ig_{\mu\nu}(q^2 - m_a^2)\delta_{ab} - i \left(g_{\mu\nu} - \frac{q_\mu q_\nu}{q^2} \right) \hat{\Sigma}_T^{ab}(q^2) - i \frac{q_\mu q_\nu}{q^2} \hat{\Sigma}_L^{ab}(q^2) \quad (4.14)$$

for $a, b = \gamma, Z$. Since the photon and the Z boson are a mixture of interaction eigenstates. By contracting the inverse propagator with the polarisation vector $\epsilon^\nu(q)$, the condition for the

longitudinal component is automatically fulfilled as demanded by the Ward identity, whereas the transversal components lead to the conditions:

$$\operatorname{Re} \hat{\Sigma}_T^W(m_W^2) = 0, \quad 0 = \operatorname{Re} \left. \frac{\partial \hat{\Sigma}_T^W(q^2)}{\partial q^2} \right|_{q^2=m_W^2} \quad (4.15)$$

$$\operatorname{Re} \hat{\Sigma}_T^{ZZ}(m_Z^2) = 0, \quad 0 = \operatorname{Re} \left. \frac{\partial \hat{\Sigma}_T^{ZZ}(q^2)}{\partial q^2} \right|_{q^2=m_Z^2} \quad (4.16)$$

$$\operatorname{Re} \hat{\Sigma}_T^{\gamma Z}(0) = 0, \quad 0 = \operatorname{Re} \left. \frac{\partial \hat{\Sigma}_T^{\gamma Z}(q^2)}{\partial q^2} \right|_{q^2=0} \quad (4.17)$$

$$\operatorname{Re} \hat{\Sigma}_T^{\gamma\gamma}(0) = 0, \quad 0 = \operatorname{Re} \left. \frac{\partial \hat{\Sigma}_T^{\gamma\gamma}(q^2)}{\partial q^2} \right|_{q^2=0} \quad (4.18)$$

In order for the Higgs fields to retain their stationary points at the predefined values v_i , the tadpole conditions defined in Eq. (3.18) must also be fulfilled in higher order calculations. However, since the fields are shifted by contributions \hat{T}_{h_i} from the tadpole diagrams shown in Fig. 4.3, the counterterms δt_{h_i} must be chosen such, that both the divergent and finite parts cancel:

$$T_{h_i}^{\text{nl}} + \delta t_{h_i} = 0. \quad (4.19)$$

Hence, the tadpole diagrams can be omitted in higher order amplitudes, as their contribution vanishes.



Figure 4.3.: Generic next-to-leading order tadpole contributions to the scalar Higgs fields h_i . F , S , U , and V represent arbitrary fermionic, scalar, ghost and vector fields, respectively.

Renormalisation conditions for fermionic propagators can be formulated in a similar way. They are however more complicated due to their Lorentz structure. In this thesis it is not necessary to exploit any fermionic renormalisation conditions, as all quantities required for Higgs phenomenology of the CP conserving NMSSM at next-to-leading order are functions of the set of independent parameters presented in Eq. (3.13), the counterterms of which can be determined from corrections to bosonic propagators and tadpole conditions.

4.3.4. Renormalisation Schemes

Note that the conditions given in Eq. (4.11) are more restrictive than generally required to achieve renormalisation. Whether the finite loop contributions are cancelled completely by the counterterms, or if they produce a shift in the propagator pole is a matter of definition referred to as renormalisation scheme.

The frequently used $\overline{\text{MS}}$ scheme demands, that the counterterms solely cancel the loop amplitude contributions proportional to the Δ pole of dimensional regularisation defined in Eq. (4.6). The same condition is used by the $\overline{\text{DR}}$ scheme, with the difference of regularising the loop integrals via dimensional reduction.

In contrast, the On-shell scheme additionally demands a cancellation between the finite parts of the counterterms and self-energies, so that the numerical values of physical quantities are unaffected by higher order corrections.

The choice of renormalisation scheme would not affect the results of an exact theory (i.e. when considering all orders of the perturbation series expansion), but it alters the values of observables in finite order perturbative calculations. Comparing observables in different renormalisation schemes therefore gives an estimate for the theoretical error due to unknown higher order corrections.

Higgs Vertex Renormalisation

Let us now apply the general remarks of the previous chapter to the trilinear NMSSM Higgs couplings of one scalar to two pseudoscalar Higgs bosons. The results presented in this chapter were computed using the `Mathematica` packages `FeynArts` [36], `FormCalc` and `LoopTools` [34] together with self-written `Bash` scripts and `Form` [37] routines.

5.1. Loop Diagrams

With the exception of the gluino, the masses of all NMSSM particles are generated due to couplings with the Higgs fields and eventual soft-breaking terms¹. Therefore one can expect a plethora of diagrams contributing to the one-loop correction of the Higgs self-couplings. Indeed, the most general CP conserving case yields 2102 diagrams when particles are inserted explicitly, which is why the systematical approach of an amplitude generator, such as `FeynArts`, is crucial.

Supplied with a model file, `FeynArts` determines all contributions to the desired process and, furthermore, can group the individual diagrams to generic field insertions, in which all diagrams have the same Lorentz structure. This abbreviates the calculation to nine distinct sub-processes listed in Fig. 5.1.

Using a model file automatically generated with `SARAH` [38], which contains information on the NMSSM particle content and couplings, the one-loop amplitude for the $\mathbf{h}_\alpha \rightarrow \mathbf{h}_\beta \mathbf{h}_\gamma$ decay was successfully generated. However, the subsequent regularisation and algebraic simplification could not be performed by `FormCalc`, because the explicit coupling terms of the model are too long for the program to handle. In order to solve this problem, all relevant couplings had to be substituted by generic vertex functions, which only need to reflect the index structure of the respective vertex. By giving appropriate names to the functions, it is easier to keep track of the particular contributions, as the amplitude reduces to index sums over products of two or three vertex functions weighted with a Passarino-Veltman integral and eventual constant terms.

Further problems arose, as the calculated amplitude contained partly ambiguous index structures. These implied summing twice over the same index, although the involved terms were

¹Gluino masses are completely due to the soft supersymmetry breaking terms.

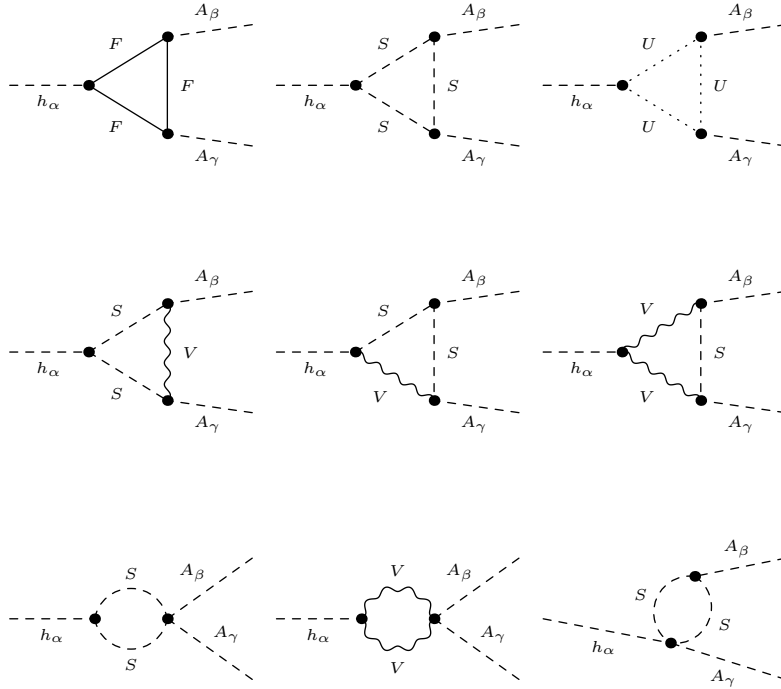


Figure 5.1.: Generic next-to-leading order contributions to the $\mathbf{h}_\alpha \mathbf{h}_\beta \mathbf{h}_\gamma$ vertex for $\alpha \in \{1, 2, 3\}$, $\beta, \gamma \in \{4, 5\}$. F , S , U , and V represent arbitrary fermionic, scalar, ghost and vector fields, respectively.

not invariant under index permutations. Since the available `FeynArts` and `FormCalc` documentation did not suggest an internal solution to this bug, the simplified amplitude had to be modified manually by a `Bash` script, which replaced the ill-defined structures and passed the expression through `Form` where the index summations were carried out. Ultimately, the resulting term was evaluated numerically by computing the involved one-loop integrals with `LoopTools` and by assigning numerical values to the explicit vertex function elements. The complete numerical evaluation was performed using `Mathematica` routines written by Kathrin Walz in the scope of her diploma thesis [39].

Despite of the abbreviative approach by generic vertex functions, the explicit computations required for the determination of the one-loop amplitude are tedious and do not yield new insights in the topic. To summarise this discussion for further calculations, we define the amplitude of the one-loop corrections displayed in Fig. 5.1 weighted with appropriate symmetry factors as

$$\mathcal{G}_{\alpha\beta\gamma}^{3\mathbf{h}} = \sum \{\text{Fig. 5.1}\} \quad (5.1)$$

In the following, expressions indexed with Greek letters α , β and γ yield for all combinations of the five Higgs boson mass eigenstates \mathbf{h}_α defined in Eq. (3.21). However, since the CP conserving NMSSM model file incorporates an alternative convention, in which the scalar and the pseudoscalar Higgs sector are treated separately, additional one-loop processes would have to be calculated for the scalar-to-scalar Higgs decays. Due to the elaborate manual index structure fixing, these contributions exceed the scope of this thesis, therefore we limit the calculations to the case

$$\alpha \in \{1, 2, 3\}, \quad \beta, \gamma = \{4, 5\}$$

5.1.1. Crosschecks

By convention, `LoopTools` cuts off the divergent parts of loop integrals by setting $\Delta = 0$, so that the previously discussed procedure should result in the finite part of the one-loop contribution to the renormalised vertex, but it would be reckless to rely on the result of such a delicate calculation without internal crosschecks. For this reason an alternative approach to the `Bash` workaround-script was developed, in which the model file vertex rules were re-substituted into the simplified amplitude, so that the index sums and numerical substitutions could be performed in terms of the original model parameters.

A further reliable strategy to verify the results is to compare the omitted divergent part of the amplitude with the corresponding counterterm divergence. For this purpose the `FormCalc` function `UVDivergentPart` can be used to isolate the contributions of the amplitude proportional to Δ , which can thereafter be numerically evaluated using the same procedure as for the finite part of the one-loop amplitude. When renormalisation was successfully achieved, the divergent next-to-leading order and counterterm parts cancelled with a precision of 10^{-10} . Ultimately, the results of the renormalisation procedure were crosschecked with independent calculations performed by Thi Nhung Dao and Kathrin Walz.

5.2. Counterterms

We have seen in Sec. 4.3.2, how the counterterm Feynman rules can formally be derived from the Lagrangian. However, for practical calculations it is more convenient to derive the counterterm in an alternative approach, in which the vertex and field renormalisation contributions are treated separately. Before these are discussed, let us define the parameter basis and specify renormalisation conditions used to determine the counterterms. The framework required for the numerical analysis at next-to-leading order described in the following section was developed by the authors of [40].

5.2.1. Parameter Basis

According to the introduction presented in Chapter ??, the Higgs sector of the CP conserving NMSSM is described by the 12 Lagrangian parameters summarised in Eq. (3.13). The subsequent analysis of the scalar Higgs potential however introduces possibilities to express these parameters in terms of quantities more convenient for phenomenological purpose:

The dependence on the soft supersymmetry breaking masses m_{H_d} , m_{H_u} , m_S can be eliminated by the tadpole conditions t_{h_u} , t_{h_d} , t_{h_s} introduced in Eq. (3.18), yielding

$$\begin{aligned} m_{H_d}^2 &= \frac{t_{h_d}}{v_d} + \frac{\lambda A_\lambda v_u v_s}{\sqrt{2} v_d} - \frac{g_1^2 + g_2^2}{8} (v_d^2 - v_u^2) - \frac{\lambda^2}{2} (v_u^2 + v_s^2) + \frac{\lambda \kappa v_u v_s^2}{2 v_d} \\ m_{H_u}^2 &= \frac{t_{h_u}}{v_u} + \frac{\lambda A_\lambda v_d v_s}{\sqrt{2} v_u} - \frac{g_1^2 + g_2^2}{8} (v_u^2 - v_d^2) - \frac{\lambda^2}{2} (v_d^2 + v_s^2) + \frac{\lambda \kappa v_d v_s^2}{2 v_u} \\ m_S^2 &= \frac{t_{h_s}}{v_s} + \frac{\lambda A_\lambda v_d v_u}{\sqrt{2} v_s} - \frac{\kappa A_\kappa v_s}{\sqrt{2}} - \frac{\lambda^2}{2} (v_d^2 + v_u^2) - \kappa^2 v_s^2 + \lambda \kappa v_d v_u. \end{aligned} \quad (5.2)$$

The vacuum expectation values v_u , v_d can be replaced by the Standard Model Higgs vacuum expectation value v and the angle t_β as

$$v_u = \frac{t_\beta v}{\sqrt{1 + t_\beta^2}}, \quad v_d = \frac{v}{\sqrt{1 + t_\beta^2}}. \quad (5.3)$$

The trilinear soft supersymmetry breaking parameter A_λ can be expressed in terms of the charged Higgs mass

$$A_\lambda = \frac{\sqrt{2} s_\beta c_\beta}{\lambda v_s} \left(\frac{m_{H^\pm}^2}{(c_{\beta_B} c_\beta + s_{\beta_B} s_\beta)^2} + \frac{\lambda^2 v^2}{\sqrt{2}} - m_W^2 \right) - \frac{\sqrt{2} (s_{\beta_B}^2 s_\beta t_{h_d} + c_{\beta_B}^2 c_\beta t_{h_u})}{\lambda v v_s (c_{\beta_B} c_\beta + s_{\beta_B} s_\beta)^2} - \frac{\kappa v_s}{\sqrt{2}}. \quad (5.4)$$

And ultimately, the Standard Model gauge couplings g_1 , g_2 and the vacuum expectation value v introduced in the above substitutions can be replaced by the electric charge e and the weak gauge boson masses m_W , m_Z

$$g_1 = \frac{e m_Z}{m_W}, \quad g_2 = \frac{e m_Z}{\sqrt{m_Z^2 - m_W^2}}, \quad v = \frac{2 m_W}{e m_Z} \sqrt{m_Z^2 - m_W^2}. \quad (5.5)$$

Remember that in the substitution rule for A_λ it is necessary to distinguish between the mixing angles β_B and β , although they coincide at tree level, as β_B originates from isolating the Goldstone modes in the Higgs sector and is therefore treated as a rotation matrix element, which does not have to be renormalised. Likewise, the tadpole dependence cannot be eliminated by using the tree level relations $t_{h_i} = 0$ because these parameters require renormalisation.

Together with the original NMSSM potential parameters λ , κ , A_κ and v_s already introduced in Eq. (3.13), these quantities form a new parameter basis of the CP conserving NMSSM Higgs sector,

$$e, m_Z^2, m_W^2, m_{H^\pm}^2, t_{h_u}, t_{h_d}, t_{h_s}, t_\beta, \lambda, \kappa, v_s, A_\kappa. \quad (5.6)$$

The advantage of this parameter choice compared to the set originating from the Lagrangian is that the counterterms of the first seven parameters can be defined by on-shell conditions,² allowing evaluation of one-loop observables in a mixed on-shell- $\overline{\text{DR}}$ renormalisation scheme, forth on referred to as mixed scheme. Alternatively, the renormalisation conditions can be formulated in the pure $\overline{\text{DR}}$ scheme by simply omitting the final parts of the derived counterterms. The comparison of these both schemes gives a measure for the theoretical error.

5.2.2. Renormalisation Conditions

After the substitutions Eqs. (5.2)-(5.5) have been applied to the Lagrangian, the counterterm Lagrangian can be derived by replacing the bare parameters ξ_0 by the renormalised ones ξ_R and their counterterms $\delta\xi$ as already stated in Eq. (4.7),

$$\xi_0 \rightarrow \xi_R + \delta\xi, \quad \text{with } \xi \in \{\text{Eq. (5.6)}\}. \quad (5.7)$$

And likewise, the field renormalisation is realised by replacing the Higgs doublet and singlet fields by the renormalised fields according to Eq. (4.8),

$$\phi_i \rightarrow \sqrt{Z_{\phi_i}} \phi_i, \quad \text{with } \phi_i \in \{H_u, H_d, S\}. \quad (5.8)$$

The field renormalisation constants $\delta Z_{\phi_i} = Z_{\phi_i} - 1$ are determined by demanding that the residues of the renormalised propagator poles equal one. But as the mass eigenstates, to which the propagators refer, are a mixture of the interaction eigenstates, in which basis the field renormalisation constants are defined, the residue condition stated in Eq. (4.11) has to be modified by a rotation to the mass eigenstate basis,

$$\mathcal{R}_{ji}^2 \delta Z_{\phi_i} = - \left. \frac{\partial \Sigma_{\mathbf{h}_j \mathbf{h}_j}(q^2)}{\partial q^2} \right|_{q^2=m_{h_j}^2}^{\text{div}} \quad \text{with } i, j \in \{1, 2, 3\}, \quad (5.9)$$

which, due to the summation over i , is a linear system of three equations for the three constants δZ_{ϕ_i} , depending on the rotation matrix elements \mathcal{R}_{ij} defined in Eq. (3.28). The

²The tadpole parameters are not on-shell parameters in strict sense of the word, but their renormalisation conditions also define the finite counterterm part.

expression is to be evaluated at the corresponding tree level propagators mass. The identity yields for the divergent part, so that the field counterterms are defined via $\overline{\text{DR}}$ conditions.

The renormalisation conditions for the gauge boson masses m_W , m_Z and the electric charge e are defined analogously to the Standard Model as discussed in numerous textbooks and other publications, e.g. [41]. Since the gauge group is not affected by the supersymmetric extension, the only difference to the Standard Model calculation lies within the additional loop contributions from the particles introduced through the NMSSM.

For the gauge boson masses, the counterterms are given by

$$\delta m_Z^2 = \text{Re } \Sigma_T^{ZZ}(m_Z^2), \quad \delta m_W^2 = \text{Re } \Sigma_T^W(m_W^2). \quad (5.10)$$

Whereas the electric charge renormalisation condition demands the corrections to vanish in the Thomson limit, i.e. in the limit of elastic electron-photon scattering, leading to the counterterm³ δe being related to the transverse self-energies of the photon and the Z boson defined in Eq. (4.14) as

$$\delta e = e \frac{s_W}{c_W} \frac{\Sigma_T^{\gamma Z}(0)}{m_Z^2} + \frac{e}{2} \left. \frac{\partial \Sigma_T^{\gamma\gamma}(q^2)}{\partial q^2} \right|_{q^2=0}, \quad (5.11)$$

where s_W , c_W are trigonometric functions of the Weinberg angle introduced in Sec. 2.4.

The charged Higgs boson mass counterterm can likewise be determined through the on-shell condition

$$\delta m_{H^\pm}^2 = \text{Re } \Sigma_{H^\pm H^\mp}(m_{H^\pm}^2). \quad (5.12)$$

The remaining three on-shell-like tadpole renormalisation conditions demand the one-loop contributions from diagrams shown in Fig. 4.3 to vanish entirely. As the tadpole conditions are defined in the interaction basis, whereas the diagram contributions come from mass eigenstates, it is again necessary to transform the condition into the same basis, yielding

$$\delta t_{h_i} = \mathcal{R}_{ji} T_{h_j}^{\text{tlo}}, \quad i \in \{d, u, s\}, j \in \{1, 2, 3\}. \quad (5.13)$$

The renormalisation of t_β is performed in the $\overline{\text{DR}}$ scheme. As t_β is defined by the ratio of v_u and v_d , its renormalisation condition can be connected with the counterterms of the up- and down-type Higgs fields,

$$\delta t_\beta = t_\beta \left[\frac{1}{2} (\delta Z_{H_u} - \delta Z_{H_d}) + \left(\frac{\delta v_u}{v_u} - \frac{\delta v_d}{v_d} \right) \right]_{\text{div}}.$$

The one-loop analysis of the MSSM has shown [42] that the divergent behaviour of $\delta v_u/v_u$ and $\delta v_d/v_d$ is equal, so that these terms cancel in the above equation, yielding

$$\delta t_\beta = \frac{t_\beta}{2} (\delta Z_{H_u} - \delta Z_{H_d}). \quad (5.14)$$

So far we have managed to define renormalisation conditions for eight of the twelve Higgs sector parameters, without having to use a single condition based on the position of the Higgs propagator poles. These can now be used to determine the remaining four counterterms. The $\overline{\text{DR}}$ renormalisation condition for scalar propagators reads

$$\mathcal{R}_{ij} \mathcal{R}_{ik} (\delta \mathcal{M}_1)_{jk} = \text{Re } \Sigma_{\mathbf{h}_i \mathbf{h}_i}(m_{\mathbf{h}_i}^2) \Big|_{\text{div}}, \quad i, j, k \in \{1, \dots, 6\}$$

³The electric charge counterterm is alternatively introduced as $e_0 \rightarrow e_R + \delta Z_e$. Both conventions are connected by the relation: $\delta e = e \delta Z_e$.

where the varied interaction basis mass matrix $\delta\mathcal{M}_1$ is a function of the bare parameters and the counterterms and therefore also involves the four unknown counterterms $\delta\lambda$, $\delta\kappa$, δv_s and δA_κ . These can be determined by solving a linear system of equations set up by conditions for four of the five mass eigenstates

$$\mathcal{R}_{ij}\mathcal{R}_{ik}(\delta\mathcal{M}_1)_{jk} = \text{Re}\Sigma_{\mathbf{h}_i\mathbf{h}_i}(m_{\mathbf{h}_i}^2)\Big|_{\text{div}} \quad i \in \{1, \dots, 4\}, \quad (5.15)$$

yielding complicated analytic relations for the counterterms, which, however, can easily be solved with numerical routines.

5.2.3. Vertex Renormalisation Contributions

The starting point for the derivation of the vertex counterterm contributions is the tree level trilinear vertex function $\mathbf{g}_{\alpha\beta\gamma}^{3\mathbf{h}}$ defined in Eq. (3.35). As the vertex function has been derived directly from the Lagrangian, the substitutions Eqs. (5.2)-(5.5) must be applied to express the vertex function in terms of the previously discussed parameter set

$$\mathbf{g}_{\alpha\beta\gamma}^{3\mathbf{h}} \xrightarrow{(5.2)-(5.5)} \tilde{\mathbf{g}}_{\alpha\beta\gamma}^{3\mathbf{h}}. \quad (5.16)$$

Since formally only the $\delta\mathcal{L}$ contributions linear in the counterterms $\delta\xi_i$ cancel the divergences of the next-to-leading order diagrams, the vertex counterterm can be obtained by varying the tree level vertex function with respect to the model parameters defined in Eq. (5.7),

$$\delta\tilde{\mathbf{g}}_{\alpha\beta\gamma}^{3\mathbf{h}} = \sum_i \frac{\partial\tilde{\mathbf{g}}_{\alpha\beta\gamma}^{3\mathbf{h}}}{\partial\xi_i} \delta\xi_i. \quad (5.17)$$

Thus, in the mixed renormalisation scheme, the vertex counterterm contributes to both the divergent and the finite part of the one-loop amplitude, formally

$$\delta\tilde{\mathbf{g}}_{\alpha\beta\gamma}^{3\mathbf{h}} = \delta\tilde{\mathbf{g}}_{\alpha\beta\gamma}^{3\mathbf{h}}\Big|_{\text{div}} + \delta\tilde{\mathbf{g}}_{\alpha\beta\gamma}^{3\mathbf{h}}\Big|_{\text{fin}}. \quad (5.18)$$

5.2.4. Field Renormalisation Contributions

The counterterm contributions from field renormalisation cannot be included according to Eq. (5.17), as the vertex function is not explicitly dependent on the fields and defined in the mass eigenstate basis, whereas the field renormalisation counterterms are included for the interaction fields. The field renormalisation contributions $\delta\mathbf{G}_{\alpha\beta\gamma}^{3\mathbf{h}}$ can be derived from the field counterterm contributions (Eq. (5.8)) of the scalar Higgs potential introduced in Eq. (3.20) as

$$\frac{1}{2}\Gamma_1^{ijk} \left(\delta Z_{\phi_i} \phi_i \phi_j \phi_k + \phi_i \delta Z_{\phi_j} \phi_j \phi_k + \phi_i \phi_j \delta Z_{\phi_k} \phi_k \right) \in V_{\text{H,ct}}.$$

Note that the fields ϕ_i are defined as components of the six dimensional interaction field multiplet, therefore we must expand the definition of δZ_{ϕ_i} to $i \in \{4, \dots, 6\}$. Since according to Eq. (5.8) the field renormalisation constants are defined for the respective Higgs doublet fields, they must be identical for the scalar and the pseudoscalar components of a doublet, yielding

$$\delta Z_{\phi_i} = \delta Z_{\phi_{i-3}} \quad i \in \{4, \dots, 6\} \quad (5.19)$$

Hence, rotating to the mass eigenstate basis results in

$$\delta\mathbf{G}_{\alpha\beta\gamma}^{3\mathbf{h}} = \frac{1}{2} \sum_{i=1}^6 \left(\delta\mathcal{Z}_{\alpha i} \mathbf{g}_{i\beta\gamma}^{3\mathbf{h}} + \delta\mathcal{Z}_{\beta i} \mathbf{g}_{\alpha i\gamma}^{3\mathbf{h}} + \delta\mathcal{Z}_{\gamma i} \mathbf{g}_{\alpha\beta i}^{3\mathbf{h}} \right), \quad (5.20)$$

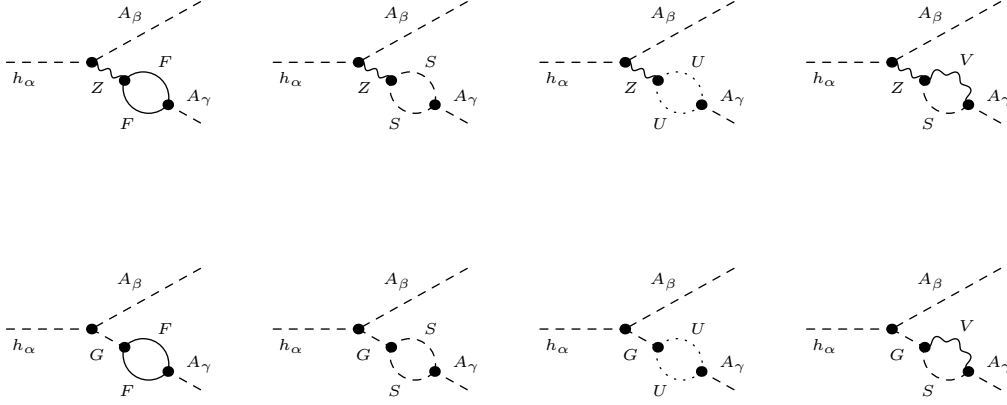


Figure 5.2.: Generic Feynman diagrams for the Z and Goldstone boson transition contributions to the one-loop $\mathbf{h}_\alpha \rightarrow \mathbf{h}_\beta \mathbf{h}_\gamma$ decay.

where $\delta\mathcal{Z}$ is the field renormalisation matrix in the mass eigenstate basis,

$$\delta\mathcal{Z}_{\alpha\beta} = \sum_i \mathcal{R}_{\alpha i} \mathcal{R}_{\beta i} \delta Z_{\phi_i}. \quad (5.21)$$

Since field renormalisation constants are defined in the $\overline{\text{DR}}$ scheme, their contribution to the vertex counterterm is pure divergent.

In conclusion, the vertex renormalisation contributions $\mathbf{g}_{\alpha\beta\gamma}^{3\mathbf{h},\text{nlo}}$ to the one-loop corrected amplitude of the $\mathbf{h}_\alpha \rightarrow \mathbf{h}_\beta \mathbf{h}_\gamma$ decay can be summarised as the sum of the one-loop diagrams introduced in Eq. (5.1) and the vertex and field renormalisation counterterms defined in Eq. (5.17) and Eq. (5.20), respectively,

$$\mathbf{g}_{\alpha\beta\gamma}^{3\mathbf{h},\text{nlo}} = \mathcal{G}_{\alpha\beta\gamma}^{3\mathbf{h}} + \delta\tilde{\mathbf{g}}_{\alpha\beta\gamma}^{3\mathbf{h}} + \delta\mathbf{G}_{\alpha\beta\gamma}^{3\mathbf{h}}. \quad (5.22)$$

5.3. Z and Goldstone Boson Transitions

So far we have only considered one-loop corrections to the Higgs vertex. However, there are additional one-loop contributions to the $\mathbf{h}_\alpha \rightarrow \mathbf{h}_\beta \mathbf{h}_\gamma$ decay due to the possibility of loop induced transition between the Z boson and the pseudoscalar Higgs bosons \mathbf{h}_γ , half of which⁴ is seen in Fig. 5.2. For reasons of gauge invariance, the Goldstone mode $G \equiv \mathbf{h}_6$ has to be treated equally. Both amplitudes can be written as products of the corresponding vertex \mathbf{g}^X with the free propagator S_X and the renormalised transition amplitude $\hat{\Sigma}_X$,

$$\mathcal{T}_{\alpha\beta\gamma}^X = 2\mathbf{g}_{\alpha\beta}^{\mathbf{h}\mathbf{h}^X} \times S_X(k^2) \times \underbrace{(\Sigma_{X\mathbf{h}_\gamma}^{\text{ct}}(k^2) + \Sigma_{X\mathbf{h}_\gamma}^{\text{nlo}}(k^2))}_{\hat{\Sigma}_X}, \quad X = G, Z. \quad (5.23)$$

The counterterm for the Z boson transition is derived from the kinetic part of the Lagrangian, yielding

$$\mathcal{L}_{Z\mathbf{h}_\gamma}^{\text{ct}} = \sqrt{g_1^2 + g_2^2} (\mathcal{R}_{4\gamma} v_d - \mathcal{R}_{5\gamma} v_u) Z^\mu \partial_\mu \mathbf{h}_\gamma \xrightarrow{(5.2)-(5.5), (5.16)} \Sigma_{Z\mathbf{h}_\gamma}^{\text{ct}} = k_\mu \hat{\Sigma}_{Z\mathbf{h}_\gamma}^{\text{ct}} \quad (5.24)$$

⁴The other half has the same structure with the transition correction connected to the propagator of A_β . These graphs are taken into account by the overall factor 2 in Eq.(5.23)

where the dependence from the momentum of the final state Higgs boson, k_μ , has been factorised out. Contracting the counterterm with the Higgs- Z -vertex via the Z boson propagator in the 't Hooft-Feynman gauge and eliminating the momentum dependence by on-shell conditions for the external particles, results in the full counterterm being of the form⁵

$$\mathcal{T}_{\alpha\beta\gamma}^{Z,\text{ct}} = 2i \mathbf{g}_{\alpha\beta}^{\text{hhZ}} \frac{m_{h_\alpha}^2 - m_{A_{\beta'}}^2}{m_{A_{\gamma'}}^2 - m_Z^2} \overset{\circ}{\Sigma}_{Z\mathbf{h}_\gamma}^{\text{ct}}. \quad (5.25)$$

The Goldstone transition originates from the variation of the Higgs boson mass matrix. With $\delta\mathcal{Z}$ defined in Eq. (5.21) and $\delta\mathcal{M}_1$ being the variation of the Higgs mass matrix in the interaction basis introduced in Eq. (3.20), the counterterm reads

$$\Sigma_{G\mathbf{h}_\gamma}^{\text{ct}} = k^2 \delta\mathcal{Z}_{6\gamma} - \frac{1}{2} m_{A_{\gamma'}}^2 \delta\mathcal{Z}_{6\gamma} - (\mathcal{R}\delta\mathcal{M}_1\mathcal{R}^T)_{6\gamma}, \quad (5.26)$$

where k^2 is the momentum squared of the final state Higgs boson. The momentum dependence can likewise be eliminated by the on-shell condition⁶, yielding

$$\mathcal{T}_{\alpha\beta\gamma}^{G,\text{ct}} = \frac{2i \mathbf{g}_{\alpha\beta 6}^{\text{hhh}}}{m_{A_{\gamma'}}^2 - m_Z^2} \left(m_{A_{\gamma'}}^2 \delta\mathcal{Z}_{6\gamma} - \frac{1}{2} m_{A_{\gamma'}}^2 \delta\mathcal{Z}_{6\gamma} - (\mathcal{R}\delta\mathcal{M}_1\mathcal{R}^T)_{6\gamma} \right) \quad (5.27)$$

Thus, together with the divergent one-loop contributions calculated in analogy to the vertex contributions in Eq. (5.1), the complete transition contributions $\mathcal{T}_{\alpha\beta\gamma}^G$, $\mathcal{T}_{\alpha\beta\gamma}^Z$ can be determined.

5.4. Mass Corrections

As shown in [40, 43], one-loop corrections can have a considerable impact on the Higgs boson masses and thereby also on the Higgs-to-Higgs decays. The kinematic constraint for on-shell $\mathbf{h}_\alpha \rightarrow \mathbf{h}_\beta \mathbf{h}_\gamma$ decays,

$$m_{h_\alpha} > m_{A_{\beta'}} + m_{A_{\gamma'}}, \quad (5.28)$$

can either be violated or fulfilled due to one-loop effects, depending on how large the corrections for the particular masses turn out. For this reason, it is sensible to abandon the strict one-loop treatment of the process and incorporate additional mass corrections to the initial and final state Higgs bosons, whereas the masses occurring in the internal propagators retain their tree level values. The external masses can be set to their one-loop values with the `FeynArts` function `OffShell`,

$$m_{h_\alpha}^2, m_{A_{\beta'}}^2, m_{A_{\gamma'}}^2 \xrightarrow{\text{OffShell}} m_{h_\alpha}^{2\text{ll}}, m_{A_{\beta'}}^{2\text{ll}}, m_{A_{\gamma'}}^{2\text{ll}}. \quad (5.29)$$

Additionally, it is necessary to replace the rotation matrix \mathcal{R} defined in Eq. (3.28) with its one-loop equivalent $\mathcal{R}^{1\text{ll}}$,

$$\mathcal{R} \xrightarrow{\text{OffShell}} \mathcal{R}^{1\text{ll}}, \quad (5.30)$$

which transforms the interaction eigenstates directly into the one-loop corrected mass eigenstates,

$$\mathbf{h}^{1\text{ll}} = \mathcal{R}^{1\text{ll}} \boldsymbol{\phi} = (h_1^{1\text{ll}}, h_2^{1\text{ll}}, h_3^{1\text{ll}}, A_1^{1\text{ll}}, A_2^{1\text{ll}}, G), \quad (5.31)$$

$$\mathcal{R}^{1\text{ll}} \mathcal{M}_1 (\mathcal{R}^{1\text{ll}})^T = \text{diag}(m_{h_1}^{2\text{ll}}, m_{h_2}^{2\text{ll}}, m_{h_3}^{2\text{ll}}, m_{A_1}^{2\text{ll}}, m_{A_2}^{2\text{ll}}, 0). \quad (5.32)$$

⁵To retain consistent index structures for the pseudoscalar Higgs masses, we define primed indices for the masses as $\beta' = \beta - 3$, $\gamma' = \gamma - 3$.

⁶The terms proportional to $m_{A_{\gamma'}}^2$ are not simplified on purpose, as they are treated separately in the subsequent chapter. Only the mass term originating from the squared momentum is replaced with the one-loop mass.

By applying the mass substitutions to the previously introduced tree level vertex Eq. (3.35), the one-loop corrected amplitude Eq. (5.22) and to the transition contributions⁷ Eq. (5.23),

$$\mathbf{g}_{\alpha\beta\gamma}^{3\mathbf{h}} \xrightarrow{(5.30)} \bar{\mathbf{g}}_{\alpha\beta\gamma}^{3\mathbf{h}} \quad (5.33)$$

$$\left. \begin{array}{l} \mathbf{g}_{\alpha\beta\gamma}^{3\mathbf{h},\text{nlo}} \\ \mathcal{T}_{\alpha\beta\gamma}^{G/Z} \end{array} \right\} \xrightarrow{(5.29),(5.30)} \left\{ \begin{array}{l} \bar{\mathbf{g}}_{\alpha\beta\gamma}^{3\mathbf{h},\text{nlo}} \\ \bar{\mathcal{T}}_{\alpha\beta\gamma}^{G/Z} \end{array} \right. \quad (5.34)$$

the complete computation of the mass corrected, renormalised $\mathbf{h}_\alpha \rightarrow \mathbf{h}_\beta \mathbf{h}_\gamma$ decay amplitude $\mathcal{A}_{\alpha\beta\gamma}^{\text{nlo}}$ can be summarised as,

$$\mathcal{A}_{\alpha\beta\gamma}^{\text{nlo}} = \bar{\mathbf{g}}_{\alpha\beta\gamma}^{3\mathbf{h}} + \bar{\mathbf{g}}_{\alpha\beta\gamma}^{3\mathbf{h},\text{nlo}} + \bar{\mathcal{T}}_{\alpha\beta\gamma}^{G/Z}. \quad (5.35)$$

⁷According to the remarks in the previous footnote, prudence is called for in substituting the pseudoscalar masses in the counterterm, as only the mass dependence originating from the on-shell condition $k^2 = m^2$ is to be substituted by the one-loop corrected values, whereas the contributions originating from the mass matrix entries are kept at their tree level value.

6.1. Scenario Search

The original motivation for the analysis developed in this thesis were the known complications in establishing a no-lose theorem for the NMSSM Higgs boson discovery at the LHC [44–46], for which scenarios with allowed $h_\alpha \rightarrow A_1 A_1$ decays are one of the main reasons. It is therefore an interesting, yet up to now an uninvestigated, question, in which way the inclusion of one-loop corrections to the Higgs self-coupling would affect the predictions for the detection potential of the LHC.

Recent ATLAS [47] and CMS [48] Higgs search results, however, imply a Standard Model-like Higgs signal in the mass region of $\sim 124\text{--}126$ GeV with a local statistical significance of 3.5σ and 3.1σ , respectively. If the signal does not turn out to be a statistical fluctuation, this would resolve the no-lose theorem difficulties instantaneously, which is why we have decided to redirect our attention to phenomenological consequences of the $h_\alpha \rightarrow A_1 A_1$ corrections in scenarios with a Standard Model-like Higgs boson of mass around 125 GeV. Note that this choice scenario implies several constraints, as it requires

- The Standard Model-like Higgs boson h_{SM} should be one of the scalar NMSSM Higgs bosons with $120\text{GeV} \leq m_{h_{\text{SM}}} \leq 130\text{GeV}$.
- To ensure Standard Model-like production and decay rates, the couplings of h_{SM} to the Z and W bosons and the top and bottom quarks should differ by no more than $\tilde{25}\%$ from the corresponding Standard Model Higgs coupling.
- In order to retain the Standard Model signal, h_{SM} must additionally have Standard Model-like branching ratios, which means that h_{SM} should not be able to decay into any particles introduced through the supersymmetric extension, or, respectively, these decay channels should be suppressed. Otherwise the branching ratios of the standard Higgs search channels might be significantly modified.
- Apart from the previous Standard Model Higgs criteria, we require the $h_\alpha \rightarrow A_1 A_1$ channel to be of relevance for the scenario. This means that at least the next-to-lightest scalar Higgs boson h_2 should be able to decay into two light pseudoscalar Higgs bosons A_1 , yielding $m_{h_2} \geq 2m_{A_1}$.

These criteria are highly restrictive, as on the one hand, we require the Higgs spectrum to have a light pseudoscalar A_1 allowing $h_2 \rightarrow A_1 A_1$ decays, on the other hand, the branching ratios of h_{SM} should not be affected by the presence of the light A_1 . Desired scenarios, thus, involve mass hierarchies¹:

- $m_{h_1} = m_{h_{\text{SM}}} < 2m_{A_1} \leq m_{h_2}$, where the decay width $\Gamma_{h_2 \rightarrow A_1 A_1}$ receives notable corrections through the one-loop corrected coupling.
- $2m_{A_1} \leq m_{h_1} < m_{h_2} = m_{h_{\text{SM}}}$, where the one-loop corrections to the $\Gamma_{h_1 \rightarrow A_1 A_1}$ have an impact on the detection potential for h_1 .

The second kind of scenarios involves difficulties, due to the presence of the $h_{\text{SM}} \rightarrow A_1 A_1$ decay channel, which, in general, can modify the branching ratios of h_{SM} significantly.

6.2. Parameter Scan Procedure

The starting point for the search of an appropriate scenario was a random scan over the Higgs sector parameters λ , κ , A_λ , A_κ , t_β and μ_{eff} ² within the ranges,

$$\begin{aligned} \lambda &\in [10^{-4}, 0.75] & A_\lambda &\in [-1000 \text{ GeV}, 1000 \text{ GeV}] \\ \kappa &\in [-0.65, 0.65] & A_\kappa &\in [-1000 \text{ GeV}, 1000 \text{ GeV}] \\ t_\beta &\in [1.6, 50] & \mu_{\text{eff}} &\in [150 \text{ GeV}, 200 \text{ GeV}]. \end{aligned} \quad (6.1)$$

In order to for the perturbation theory to be valid up to the GUT scale, λ and κ must not be chosen too large. In the subsequently analysed scenarios, attention was paid that the constraints on these parameters given explicitly in [49] were fulfilled. The scan points were assigned using the `Bash` function `$random` which generates a random integer between 0 and 23767. Therefore each of the intervals in (6.1) was divided into 23768 equidistant values, from which one was picked by the `$random` function. Mathematically this procedure is described by,

$$\rho = \rho_{\text{min}} + [\rho_{\text{max}} - \rho_{\text{min}}] p_\rho \quad \text{with } \rho = \lambda, \kappa, A_\lambda, A_\kappa, \mu_{\text{eff}},$$

where p_ρ is the normalised random number. During the scan procedure the results showed that small values of t_β were preferable³. Therefore the generator formula was adjusted to prefer small values, by using

$$t_\beta = t_{\beta\text{min}} + [t_{\beta\text{max}} - t_{\beta\text{min}}] p_{t_\beta}^3.$$

The tadpole parameters t_{h_d} , t_{h_u} , t_{h_s} were set to zero, whereas the Standard Model parameters e , m_W , m_Z were determined⁴, according to the SUSY Les Houches Accord (SLHA) conventions [50, 51], from the Fermi constant G_F , the value of the electromagnetic fine-structure constant α_{em} at the electroweak scale and the Z boson mass m_Z .

$$\begin{aligned} \text{SLHA:} & & (5.6): \\ G_F = 1.16637 \cdot 10^{-5} \text{ GeV}^{-2} & \rightarrow & m_W = 79.829 \text{ GeV} \\ m_Z = 91.1876 \text{ GeV} & & m_Z = 91.1876 \text{ GeV} \\ \alpha_{\text{em}}^{-1} = 127.934 & & e = 0.313409 \end{aligned}$$

¹In our scenarios, the decays of h_3 into $A_1 A_1$ turned out not to lead to relevant effects.

²By convention, μ_{eff} replaces the singlet vacuum expectation value v_s to ensure the effective μ -coupling to below 200 GeV, as required by tree-level naturalness arguments. Both are connected via $v_s = \sqrt{2}\mu_{\text{eff}}/\lambda$.

³This is because small values of t_β maximise the tree-level mass of the lightest Higgs boson.

⁴The conversion rules between these parameter sets can be derived from Eqs. (5.5) together with the relations $v = (\sqrt{2}G_F)^{-1/2}$ and $e = \sqrt{4\pi\alpha}$

The remaining parameters were set to fixed values. The masses of the Standard Model fermions are given in Tab. 6.1. The soft supersymmetry breaking squark masses and trilinear couplings defined in Eq. (3.11) were set to universal values for the first two generations

$$m_{\tilde{q}} = M_{\text{susy}} = 10^3 \text{ GeV}$$

$$A_{\tilde{q}} = A_0 = 2 \cdot 10^3 \text{ GeV}.$$

The masses of the squarks of the first two generations are hence of the order of 1 TeV in order to satisfy present LHC search limits for these particles [52, 53]. The masses of the third generation squarks are still allowed to be as low as about 300 GeV - 400 GeV. In order to avoid finetuning, we choose the soft supersymmetry breaking masses and trilinear couplings according to [49] to the values,

$$m_{\tilde{t}_R} = m_{\tilde{t}_L} = m_{\tilde{b}_L} = 650 \text{ GeV} \quad m_{\tilde{b}_R} = M_{\text{susy}} \quad A_{\tilde{t}} = A_{\tilde{b}} = A_0.$$

Finally, for simplicity the soft breaking masses and trilinear couplings in the slepton sector are set to

$$m_{\tilde{e}} = M_{\text{susy}}, \quad A_{\tilde{e}} = A_0.$$

The last missing parameters are the gaugino soft breaking masses,

$$M_1 = 2M_2 = 500/3 \text{ GeV}, \quad M_3 = 600 \text{ GeV},$$

as well as the renormalisation scale μ_{ren} , which has been set to,

$$\mu_{\text{ren}} = 300 \text{ GeV}.$$

Gen	m_f in GeV		
	1	2	3
u	0.0025	1.27	173.3
d	0.0050	0.101	4.19
e	$0.5110 \cdot 10^{-3}$	0.1057	1.7768

Table 6.1.: Numerical values of the fermion masses used in the analysis.

Given these input values, the program for the scanning procedure numerically diagonalised the tree-level mass matrices. If the parameter point did not yield unphysical results, such as negative eigenvalues of the Higgs boson mass matrix, the one-loop mass spectrum and counterterms were calculated using the conditions given in Sec. 5.2.2. The results were checked whether the one-loop mass spectrum involves a Standard Model-like Higgs boson and a light pseudoscalar Higgs according to the criteria described in the previous section. If these requirements were fulfilled, the program continued to calculate the one-loop corrected decay width, as well as improved tree-level decay width, as defined in App. B, and printed these out together with the input values.

This procedure was repeated for approximately 500'000 random parameter points, producing a handful of results, two of which we shall analyse in the following sections. Unfortunately, most of the points turn out to have insignificant one-loop corrections. This may be a consequence of the high amount of constraints set on the scenario, but reliable statements would demand a detailed analysis which, in views of the large number of parameters involved, is beyond the scope of this thesis. Nevertheless a few of the points which were found show interesting effects due to the one-loop corrections, two of which we shall inspect in the following sections.

The results of the above procedure were reviewed and points with promising next-to-leading order corrections were furthermore processed by a slightly modified version of the previously

introduced script, which systematically evaluated parameter points in a region around the given starting point. The complete set of information about the mass spectrum, couplings and rotation matrix elements for each step was printed out as SLHA input files, in which the tree-level decay widths $\Gamma_{h_\alpha \rightarrow A_1 A_1}$ were replaced by the improved tree-level and the full one-loop decay width, respectively. The input files were subsequently passed through a modified version of HDECAY [54, 55] developed by the group of Prof. M. Mühlleitner. HDECAY calculated the decay spectrum of the remaining channels of the parameter point and ultimately, the HDECAY output was analysed using HiggsBounds [56], which checked, whether the scenario complies with experimental constraints from LEP, Tevatron and LHC data.

In the following analysis, we estimate the theoretical error due to unknown higher order contributions by performing all calculations in two differing definitions of the third generation quark masses. In the pole quark mass scheme, the one-loop corrected NMSSM Higgs sector is evaluated with the quark masses summarised in Tab. 6.1. Alternatively, we use the running $\overline{\text{DR}}$ top and bottom quark masses, which are determined by converting the pole masses into the corresponding $\overline{\text{DR}}$ masses and by evolving these to the renormalisation scale μ_{ren} according to the Standard Model renormalisation group equations. Finally, the gluino self-energy corrections are added to the $\overline{\text{DR}}$ masses at the scale μ_{ren} .

6.3. Scenario 1

The starting point for the first scenario with promising one-loop coupling corrections is described by the parameter set,

$$\begin{aligned} \lambda = 0.55, \quad \kappa = 0.25, \quad \mu_{\text{eff}} = 171 \text{ GeV} \\ t_\beta = 1.4, \quad A_\lambda = 244, \text{ GeV} \quad A_\kappa = 30 \text{ GeV}. \end{aligned} \quad (6.2)$$

The Higgs mass spectrum of this scenario is shown in Fig. 6.1 as a function of the ratio t_β of the Higgs vacuum expectation values. As can be inferred from the figure, the mass of lightest scalar Higgs boson $\mathbf{h}_1 = h_1$ in the region of approximately⁵ 115 GeV to 125 GeV, whereas the mass of the light pseudoscalar Higgs A_1 varies between 60 GeV and 85 GeV, thereby excluding the $h_1 \rightarrow A_1 A_1$ decay channel. Thus, the aim of this analysis is the discussion of one-loop contributions to the decay of the next-to-lightest scalar Higgs h_2 . The masses of the heavy scalar and pseudoscalar Higgs bosons lie in the region around 340 GeV and are not shown separately here.

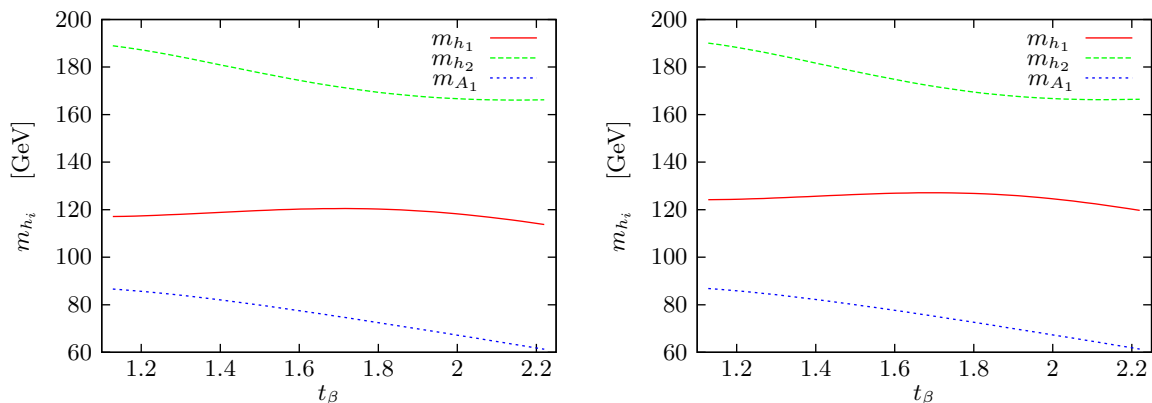


Figure 6.1.: One-loop masses of the Standard Model-like scalar Higgs boson m_{h_1} (solid), the next-to-lightest scalar Higgs boson m_{h_2} (dashed) and of the light pseudoscalar Higgs boson m_{A_1} (dotted) as functions of t_β with the running $\overline{\text{DR}}$ top and bottom quark masses (left) and with the top and bottom quark pole masses (right)

⁵The fact that this mass lies slightly under the required value is not further disturbing. We will see in the following, that when theoretical uncertainties for the mass are taken into account, the required value fairly within the mass span.

In order to estimate the theoretical error due to neglected higher-order contributions, the complete analysis was performed for pole quark masses, as described in the previous section, and for running $\overline{\text{DR}}$ top and bottom quark masses, respectively. The theoretical uncertainty on the mass of h_1 due to the quark mass renormalisation scheme turns out to be of up to 6%, whereas the uncertainties for h_2 and A_1 lie below 1%. This dependence is not further surprising when we recall that h_1 is required to have couplings comparable to the Standard Model Higgs couplings, which lead to a notable quark mass dependence of m_{h_1} due to the one-loop contributions from the heavy quarks and the corresponding squarks. We define the ratio R_X of the h_i couplings to gauge bosons and the up and down type quarks with respect to the corresponding Standard Model coupling as,

$$R_X(h_i) = \left| \frac{g_{h_i X X}^{\text{NMSSM}}}{g_{h_i X X}^{\text{SM}}} \right|^2, \quad X = W/Z, t, b, \quad (6.3)$$

which, when the couplings are inserted explicitly and the notations of the previous chapters are used, yield

$$R_d(h_i) = |\mathcal{R}_{i1}/c_\beta|^2, \quad R_u(h_i) = |\mathcal{R}_{i2}/s_\beta|^2, \quad R_{Z/W}(h_i) = |c_\beta \mathcal{R}_{i1} + s_\beta \mathcal{R}_{i2}|^2. \quad (6.4)$$

The resulting ratios $R_X(h_1)$ are displayed in the left plot of Fig. 6.2 for the running $\overline{\text{DS}}$ top and bottom masses and yield good agreement with the constraints, as they differ by less than 25% on a broad range of t_β values. The adequate plot for the pole top and bottom mass scheme yields similar examples, in which the deviation between the respective couplings does not exceed the 25% mark in a slightly smaller interval of $1.25 \leq t_\beta \leq 2.1$.

On the other hand, the small deviations of m_{A_1} and m_{h_2} due to the quark mass renormalisation scheme indicate potential high singlet contributions in the mass eigenstates, which lead to suppressed quark couplings and therefore mitigate the dependence from the quark masses. This assumption is verified in the right plot of Fig. 6.2 by the visualisation of the squared mixing matrix elements $|\mathcal{R}_{23}|^2$, $|\mathcal{R}_{46}|^2$ which are a measure for the contribution of the singlet fields $\phi_3 = h_s$, $\phi_6 = a_s$ to the mass eigenstates $\mathbf{h}_2 = h_2$, $\mathbf{h}_4 = A_1$. Thus, as the effect of the quark mass renormalisation scheme on the $h_2 \rightarrow A_1 A_1$ channel is of negligible order, we will restrict the following discussion to the $\overline{\text{DR}}$ quark mass renormalisation scheme.

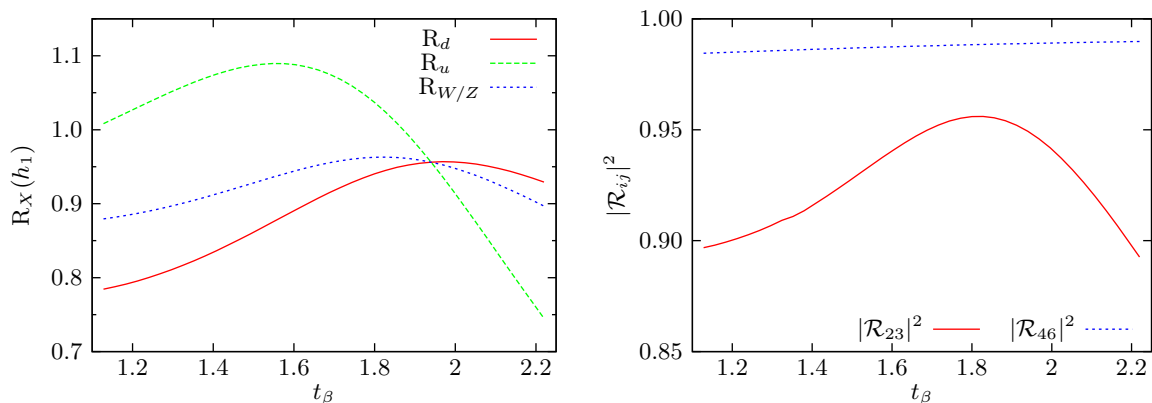


Figure 6.2.: Left: The ratio of the h_1 couplings to gauge bosons and up and down type quarks with the corresponding Standard Model couplings $R_X = |g_{h_1 X X}^{\text{NMSSM}}/g_{h_1 X X}^{\text{SM}}|^2$ as a function of t_β . Right: The squares of the Higgs boson mixing matrix elements \mathcal{R}_{23} , \mathcal{R}_{46} plotted likewise over the Higgs boson vacuum expectation value ratio t_β .

Let us now analyse the $h_2 \rightarrow A_1 A_1$ decay. As already said, the starting point parameters Eq. (6.2) yielded promising one-loop corrections to the Higgs self-coupling. Unfortunately, the

comparison of the improved tree-level and one-loop decay widths in Fig. 6.3 shows, that this relatively high correction of $\sim 17\%$ is only given for small values of t_β , where the decay widths are both small. The left diagram of Fig. 6.4 shows in detail, how the deviation between the improved tree-level and the one-loop corrected decay widths tends to zero for higher values of t_β .

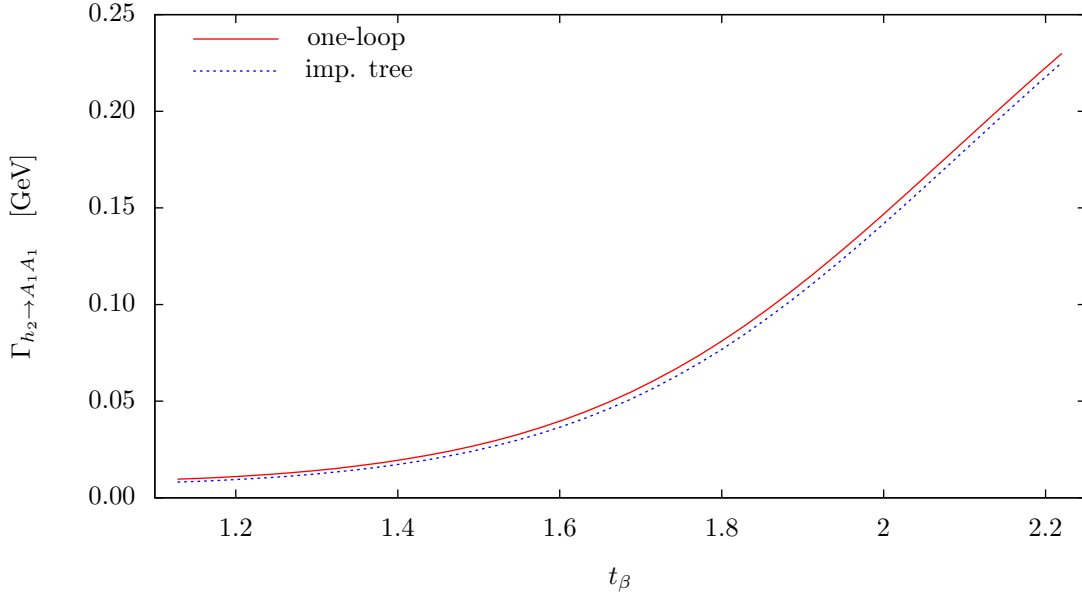


Figure 6.3.: Improved tree-level (dashed/blue) and the one-loop corrected (full/red) decay width of the next-to-lightest scalar Higgs h_2 into the light pseudoscalar Higgs bosons A_1 . The comparison yields, that the improved tree-level coupling is a good approximation for this parameter point.

Additionally, Fig. 6.5 endorses the lack of significance of the one-loop corrections, as in the low t_β region the branching ratio of the $h_2 \rightarrow A_1 A_1$ decay is suppressed due to the kinematically allowed decay into W bosons. Even though the gauge boson couplings of h_2 are weaker compared to a Standard Model Higgs of the same mass due to the high singlet contributions, the channel still yields the highest decay width. The A_1 channel starts to dominate in the t_β region, in which the singlet contribution to h_2 rises over 92%, which leads to a high suppression of the coupling to vector bosons, as can be seen in the right diagram of Fig. 6.4.

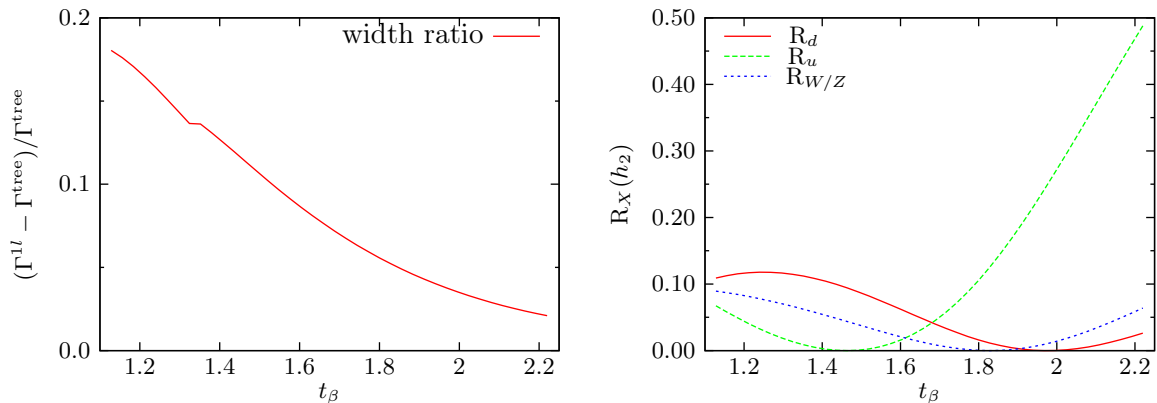


Figure 6.4.: Left: Correction of the $h_2 \rightarrow A_1 A_1$ decay width due to next-to-leading order contributions normalised to the improved tree-level decay width as a function of t_β . Right: h_2 coupling normalised to the Standard Model Higgs coupling according to Eq. 6.3.

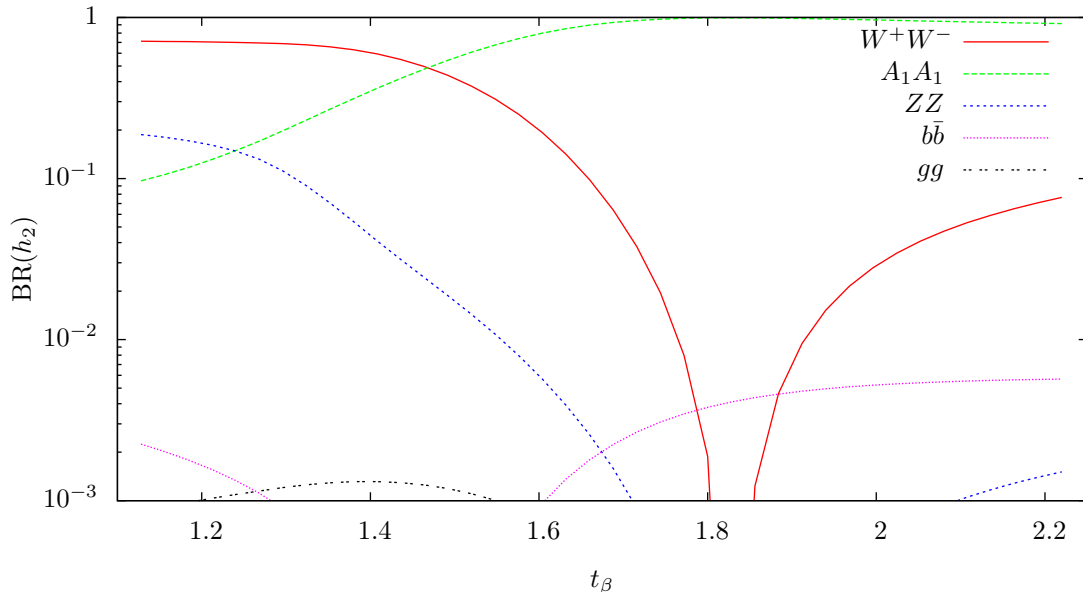


Figure 6.5.: Branching ratios of the next-to-lightest scalar Higgs boson h_2 using the one-loop corrected $h_2 A_1 A_1$ coupling plotted logarithmically over t_β . The W decay channel is highly suppressed in the region where the singlet contributions to the h_2 mass eigenstate reach $\sim 95\%$ (cf. Fig 6.2).

In conclusion, the first scenario turned out to be rather disappointing, as no noteworthy effects were introduced through the one-loop corrected Higgs self-coupling. As the vast majority of the points found through our scans yielded similarly small corrections, one might tend to expect systematics behind this trend.

A possible attempt to explain this behaviour could base on the role of the singlet contributions to the mass eigenstates involved in the coupling: Singlet-like Higgs boson couplings to quarks and gauge bosons are suppressed, which could explain, why the one-loop contributions turn out to be small. This statement, however, would require further elaborate analysis.

Nevertheless, this parameter point shows that the NMSSM still complies with the present experimental constraints on the Higgs sector and furthermore is in accordance with requirements from finetuning and perturbativity. Finally, the results of our scans show that this parameter point can be considered as being fairly representative for scenarios with a Standard Model-like h_1 and possible $h_2 \rightarrow A_1 A_1$ decays, which suggests that the improved tree-level coupling is a good approximation in such cases.

6.4. Scenario 2

The second scenario can be considered contrary to the one discussed previously. The starting point parameters were found as

$$\begin{aligned} \lambda &= 0.64, & \kappa &= 0.02, & \mu_{\text{eff}} &= 185.52 \text{ GeV} \\ t_\beta &= 4.46, & A_\lambda &= 778.1, \text{ GeV} & A_\kappa &= 17.1 \text{ GeV}. \end{aligned} \quad (6.5)$$

The starting point lies in an experimentally excluded region due to the small mass of the lightest scalar Higgs bosons h_1 and the presence of a light neutralino $\tilde{\chi}_1^0$ in the spectrum, as the signatures of such scenarios have been analysed by the OPAL collaboration [57]. However, as we will see, when the one-loop Higgs coupling corrections are included, the scenario is not excluded in a shifted region of λ .

In Fig 6.6 the Higgs boson masses are displayed in the λ range from 0.55 to 0.62. In analogy to the first scenario, the analysis is performed with both the pole quark masses and the $\overline{\text{DR}}$

running quark masses, yielding theoretical uncertainties of under 1% for the mass of the light pseudoscalar Higgs m_{A_1} and of approximately 2% and up to 3.5% for the scalar Higgs masses m_{h_1} , m_{h_2} , respectively. The masses of the heavy Higgs bosons h_3 and A_2 lie above 800 GeV and are therefore not of concern for this analysis. As already mentioned, the spectrum also involves a light neutralino $\tilde{\chi}_1^0$, the mass of which lies around 19 GeV.

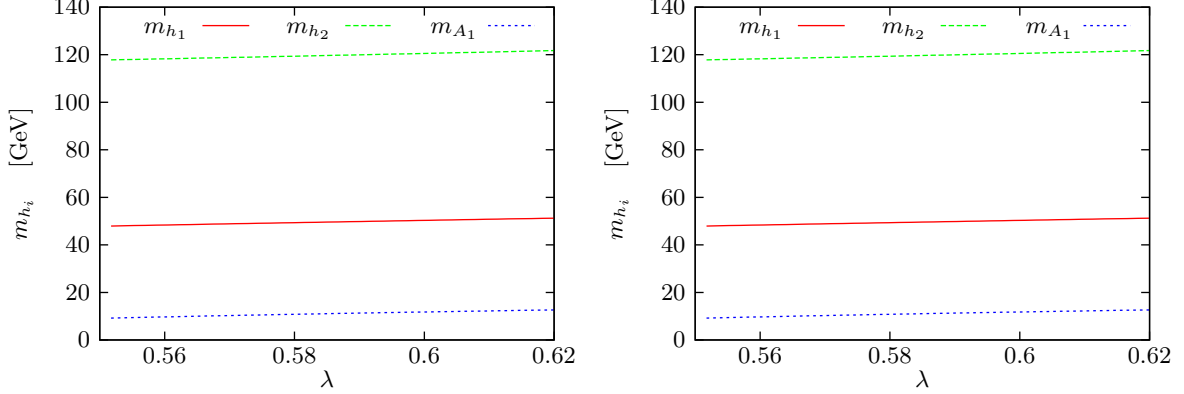


Figure 6.6.: One-loop masses of the lightest scalar Higgs boson m_{h_1} (solid), the Standard Model-like candidate Higgs boson m_{h_2} (dashed) and of the light pseudoscalar Higgs boson m_{A_1} (dotted) as functions of λ with the running $\overline{\text{DR}}$ top and bottom quark masses (left) and with the top and bottom quark pole masses (right).

The Standard Model-like candidate of this scenario is the next-to-lightest scalar Higgs boson h_2 , the mass of which lies near the desired 125 GeV when theoretical uncertainties are taken into account. We can again verify that the couplings of h_2 are comparable to the couplings of a Standard Model Higgs of the same mass according to Eq. (6.3). As can be seen in the left diagram of Fig. 6.7 for the case where the $\overline{\text{DR}}$ running quark mass was used in the calculation of the one-loop Higgs boson masses⁶, the h_2 couplings to Standard Model particles differ by no more than 20% over the whole range of λ .

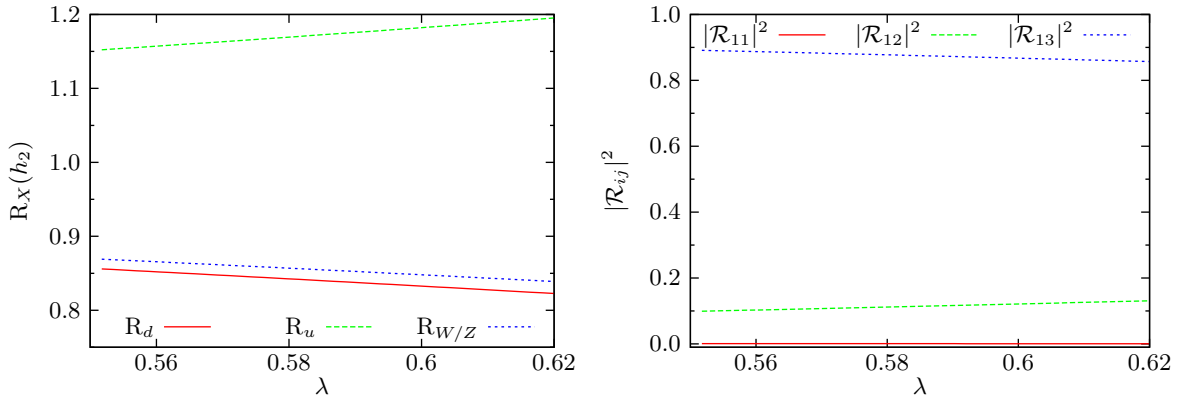


Figure 6.7.: Left: Couplings of h_2 to vector bosons and up and down type quarks normalised to the corresponding coupling of a Standard Model Higgs with the same mass. Right: Contributions of the interaction fields ϕ_d , ϕ_u , ϕ_s to the lightest scalar Higgs boson h_1 according to the \mathcal{R} matrix convention defined in Eq. (3.28). Both plots are shown for the case where $\overline{\text{DR}}$ top and bottom quark masses are used in the calculation of the one-loop Higgs masses..

In spite of these acceptable properties of h_2 , this scenario can most certainly not be used to reconstruct a Standard Model-like signal, as the spectrum involves three additional supersym-

⁶The pole quark mass scheme yields similar results.

metric particles, into which h_2 can decay. This suspicion is confirmed in Fig. 6.8, where the dominant decay channels are identified as the ones into the lightest neutralinos $\tilde{\chi}_1^0$ and into a pair of light pseudoscalar Higgs bosons A_1 . The branching ratios calculated with the pole quark masses and with the improved tree-level Higgs coupling show comparable behaviour.

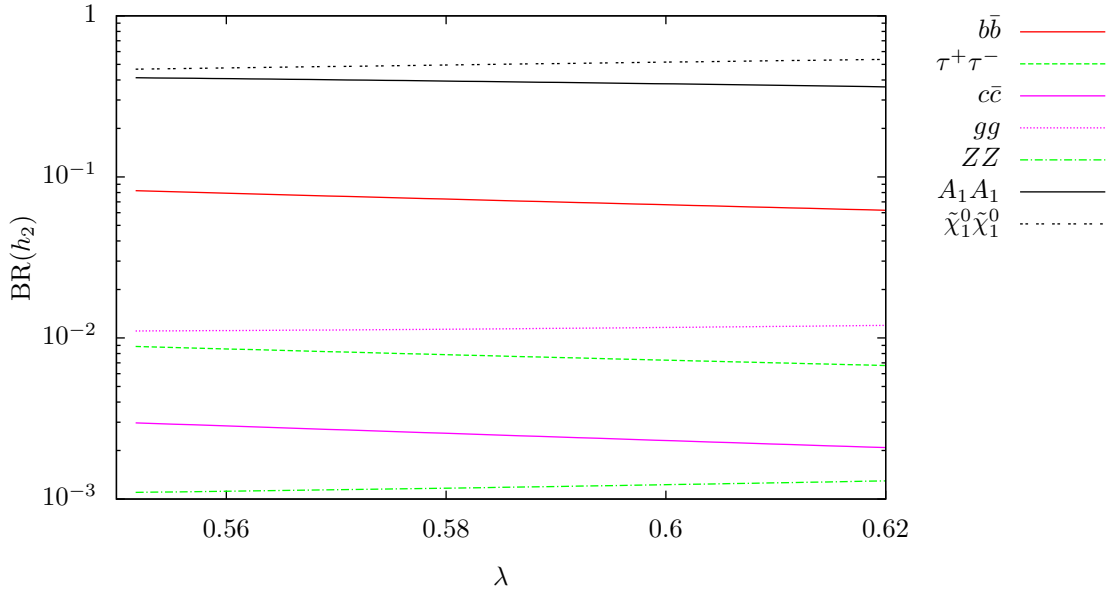


Figure 6.8.: Branching ratios of h_2 for the case where running $\overline{\text{DR}}$ top and bottom quark masses were used in the calculation of the one-loop Higgs boson masses, using the one-loop corrected $h_2 A_1 A_1$ coupling. Despite the appropriate mass and couplings, h_2 is not a suitable Standard Model-like candidate, because of the strongly differing branching ratios compared to the Standard Model. Channels with $\text{BR} < 10^{-3}$ are omitted.

The interesting feature of this scenario for our discussion is the fact, that even though all points of the parameter variation are excluded at tree-level due to the $h_1 \rightarrow \tilde{\chi}_1^0 \tilde{\chi}_1^0$ decay channel, when the improved tree-level coupling is replaced by the one-loop corrected coupling, the scenario is not excluded at the whole λ range. This is due to a high suppression of the $h_1 A_1 A_1$ improved tree-level coupling, which is compensated when the fully corrected one-loop coupling is applied. This effect is visualised in the first plot of Fig. 6.9 where we can see how, for the running $\overline{\text{DR}}$ top and bottom quark mass used in the calculation of the one-loop corrected Higgs masses, the improved tree-level decay width sinks below numerical significance for values of λ around 0.57, whereas the one-loop decay width and the improved tree-level decay width calculated using the pole quark masses, indicates no peculiar behaviour over the parameter range of $\lambda < 0.62$. The origin of the improved tree-level behaviour is difficult to determine, as the trilinear Higgs coupling is a complicated function of all Higgs sector parameters. Additionally, the rotation matrix elements \mathcal{R}_{ij} also depend on λ , and in our approach, they are calculated numerically, as the analytical forms are already at tree-level too elaborate to determine.

Even though the suppression does not seem to be caused solely by the rotation matrix elements, as, according to the right plot of Fig. 6.7, these show minimal λ dependence, they still have an effect on the suppression. This can be seen when the variation λ is expanded into the higher region, in which the scenario is forbidden even for the one-loop corrected decay width. As can be seen in the lower diagram of Fig. 6.9, the pole quark mass renormalisation scheme shows a very similar behaviour to the $\overline{\text{DR}}$ running quark mass renormalisation scheme in the region of $\lambda \approx 0.71$. Thus, the position of this cancellation effect depends on the top and bottom quark masses, which affect the Higgs self-couplings only indirectly by the one-loop

rotation matrix used to calculate the improved tree coupling. On the other hand, the one-loop corrected decay width has an additional quark mass dependence through the loop diagrams involving quarks and squarks, this dependence however leads only to a 20% deviation of the decay widths between the two quark mass renormalisation schemes used in the calculation of the one-loop Higgs masses.

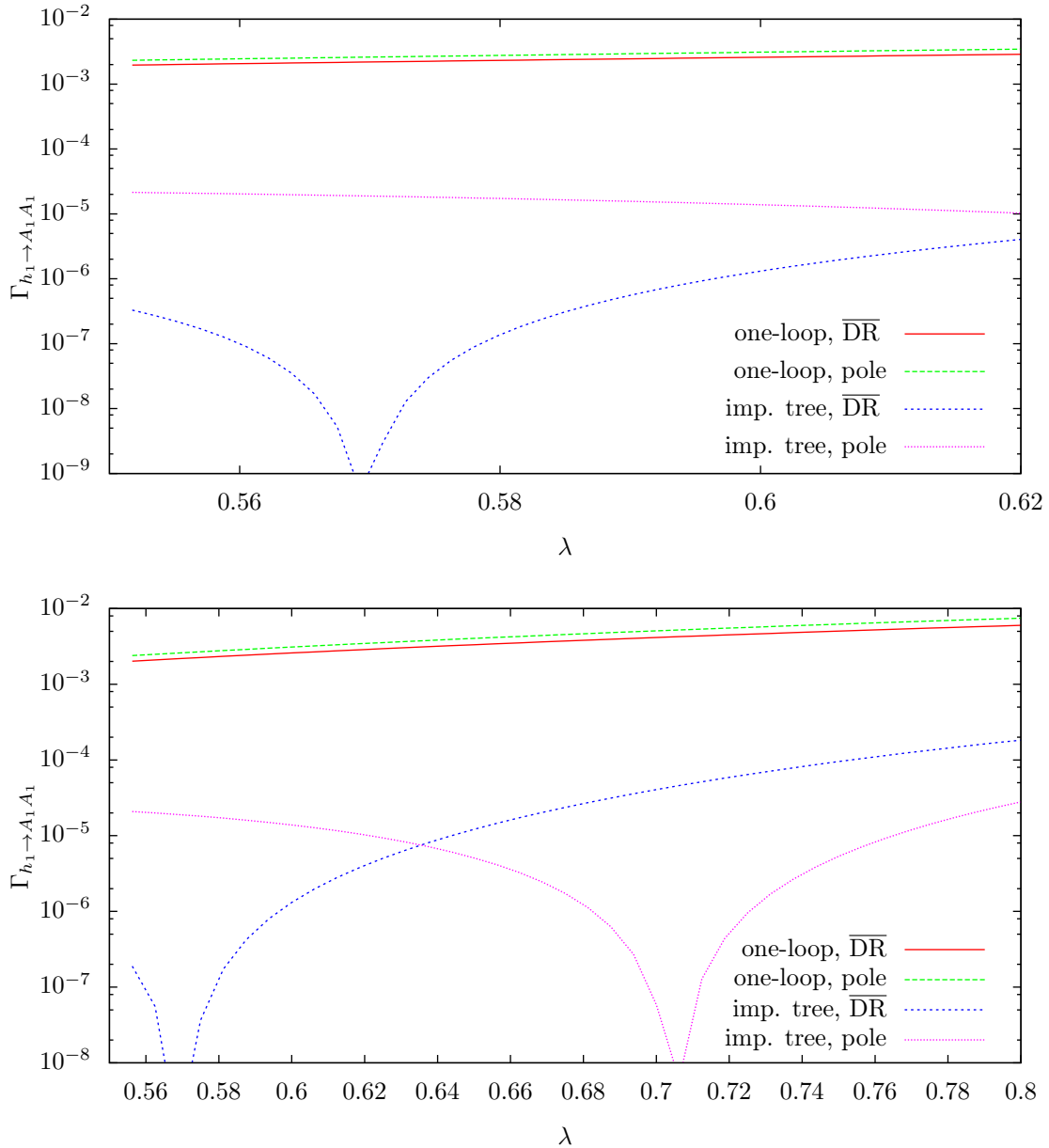


Figure 6.9.: Top: The $h_1 \rightarrow A_1 A_1$ decay width in comparison for the improved tree-level and the one-loop corrected coupling evaluated in both pole quark masses and $\overline{\text{DR}}$ running quark masses used in the calculation of the one-loop Higgs boson masses. Bottom: Same plot continued to the region $\lambda > 0.62$, in which the scenario is experimentally excluded even for the one-loop corrected decay width.

Finally, let us investigate how this vast deviation of decay widths affects the exclusion limits for this scenario. Recall that the OPAL analysis discussed in [57] is based on the production of h_1 in Higgs-strahlung and a subsequent invisible $\tilde{\chi}_1^0$ decay, resulting in a detector signature of a single Z boson and missing transverse momentum, due to the neutralinos escaping detection. When we compare the branching ratios of h_1 calculated with the improved tree-level and the

one-loop corrected Higgs coupling (cf. Fig. 6.10), we can clearly see the impact of the coupling correction on the branching ratios: For the improved tree-level coupling, the branching ratio into $\tilde{\chi}_1^0$ yields over 90%, due to the singlet nature of h_1 (cf. Fig. 6.7, right plot), with which the Standard Model decay channels cannot compare. The situation changes considerably, when the one-loop corrected Higgs coupling is applied, the branching ratio into the pseudoscalar Higgs bosons A_1 is dominant, resulting in a reduced $\tilde{\chi}_1^0$ signal, for which the OPAL exclusion criteria do not suffice.

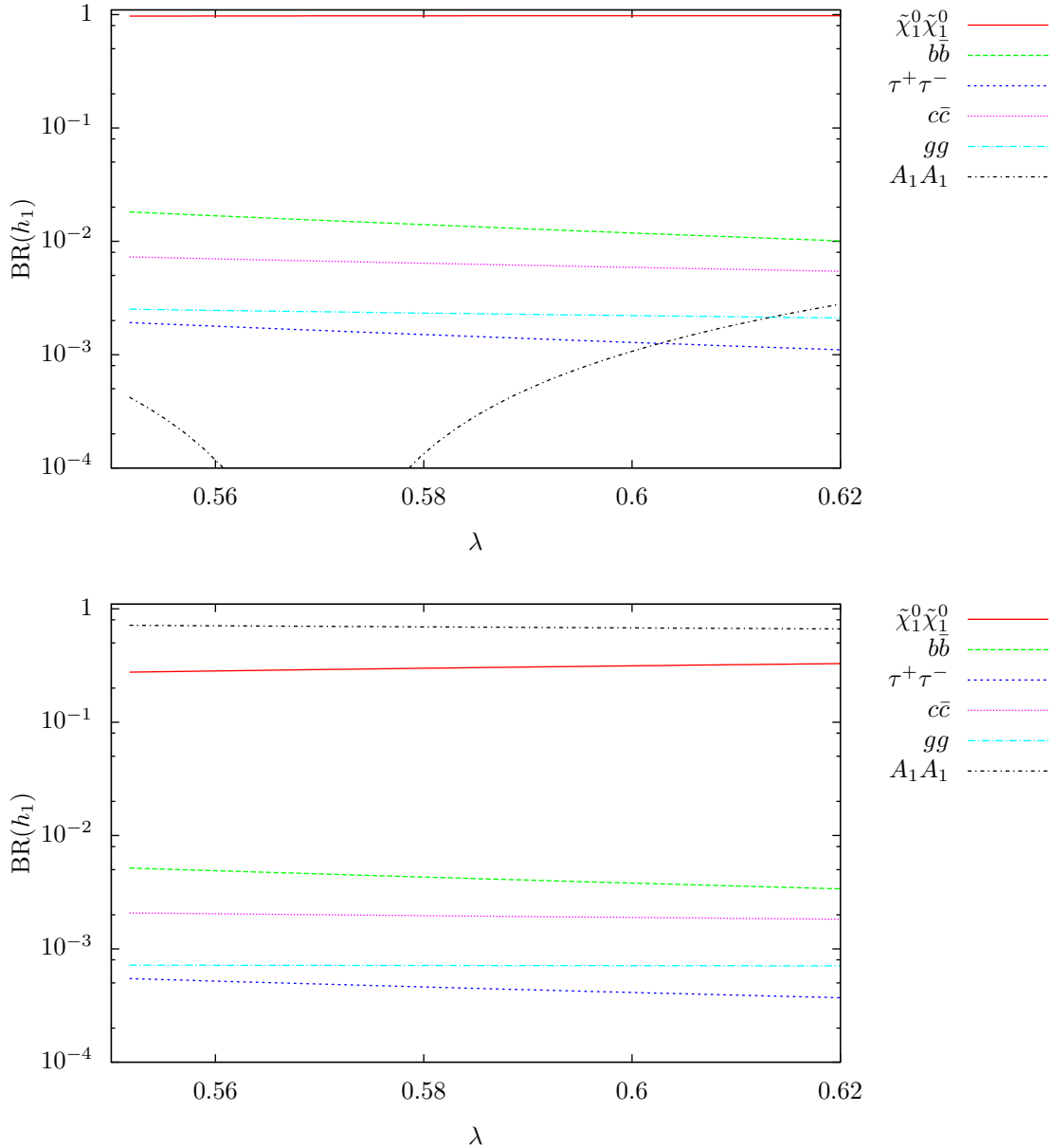


Figure 6.10.: Branching ratios of the lightest scalar Higgs boson h_1 for the improved tree-level (top plot) and the one-loop corrected (bottom plot) coupling in the $\overline{\text{DR}}$ running quark mass renormalisation scheme.

The last unsettled question of this discussion is, why the one-loop corrected decay width scenario is experimentally excluded for $\lambda > 0.62$, even though the branching ratios displayed in the bottom plot of Fig. 6.10 do not suggest any crucial alteration in that region. According to the HiggsBounds analysis, the reason for this is a gradual increase of the decay width of

the light pseudoscalar A_1 into bottom quarks, which at $\lambda = 0.62$ reaches sufficient significance for the application of the LEP exclusion limits on Higgs cascade decay described in [58].

In conclusion, the second scenario was also not fully satisfactory, as the potential Standard Model Higgs candidate h_2 cannot be used to produce a Standard Model-like Higgs signal due to the additional decay modes into light supersymmetric particles. Nevertheless, this scenario yields interesting consequences for the theoretical uncertainty estimate, as the one-loop Higgs self-coupling corrections help to avoid the λ dependent numerical cancellation of the improved tree-level $h_1 \rightarrow A_1 A_1$ decay width. Additionally, the inclusion of the one-loop corrections leads to a significant modification in the phenomenological analysis, as, even though the scenario will most likely be excluded by future LHC data, the currently available exclusion limits set up by the LEP data do not suffice to exclude the scenario in the region $0.55 < \lambda < 0.62$.

Based on the previous studies of the one-loop corrections to the NMSSM Higgs sector by the group of Prof. M. Mühlleitner, the available framework was expanded to include one-loop corrections to the CP-conserving trilinear Higgs self-coupling $h_\alpha A_\beta A_\gamma$.

In spite of initial problems caused by the large number of diagrams contributing to the one-loop amplitude, renormalisation was successfully achieved in the Feynman diagram approach using `FeynArts` for the determination of all one-loop contributions, yielding numerical cancellation for the divergent counterterm and next-to-leading order contributions up to the order of 10^{-10} for numerous random parameter points.

For subsequent phenomenological analyses a scan procedure was written, which randomly searched through the parameter space for points with allowed $h_\alpha \rightarrow A_\beta A_\gamma$ decays, that additionally involve a scalar Higgs boson in the mass region of 125 GeV with Standard Model-like couplings, in order to produce scenarios in agreement with the currently present LHC Higgs signal evidence. The scan over more than 500'000 randomly chosen points yielded several parameter points which fulfil the constraints, out of which the vast majority, however, receives insignificant corrections from the one-loop corrected self-coupling. The improved tree-level coupling shows results comparable to the one-loop corrected coupling in the most found scenarios. A representative parameter point for this sort of scenario has been discussed in section 6.3.

In contrast, the parameter point discussed in section 6.4 shows a significant change of the partial width $h_\alpha \rightarrow A_\beta A_\gamma$ due to the inclusion of one-loop corrections to the Higgs self-couplings and thereby proves, that higher order corrections can have a significant phenomenological impact and reduce the theoretical error due to unknown higher order corrections.

Going beyond the limited analysis of this thesis, further phenomenological investigations could evaluate, whether there is a systematical reason for the observed trend, that one-loop corrections to the $h_2 \rightarrow A_1 A_1$ decay are insignificant in scenarios with a Standard Model-like Higgs boson h_1 and light pseudoscalar Higgs bosons A_1 .

Ultimately, the calculation performed in the scope of this thesis serve as a source of cross-check for further projects, the aim of which is the implementation of the complete one-loop corrections to the CP-violating NMSSM trilinear Higgs self-couplings into a modified version of `HDECAY`, allowing predictions for NMSSM Higgs phenomenology with one-loop precision.

Trilinear Higgs Self-Coupling

The tree-level trilinear Higgs self-coupling has been derived in chapter 4 and was of central importance throughout the thesis, thus we present here its explicit form,

$$\begin{aligned}
\mathbf{g}_{\alpha\beta\gamma}^{\text{hhh}} = & -i(\sqrt{2}A_\lambda\lambda - 2\lambda\kappa v_S)c_\beta\mathcal{P}_{\alpha\beta\gamma}^{321}/2 - i(\sqrt{2}A_\lambda\lambda - 2\lambda\kappa v_S)\mathcal{P}_{\alpha\beta\gamma}^{421}s_\beta/2 + \\
& + iv(g_1^2 + g_2^2 - 4\lambda^2)\mathcal{P}_{\alpha\beta\gamma}^{433}s_\beta/8 + iv(g_1^2 + g_2^2 - 4\lambda^2)c_\beta\mathcal{P}_{\alpha\beta\gamma}^{344}/8 + \\
& + i(\sqrt{2}A_\lambda\lambda + 2\lambda\kappa v_S)\mathcal{P}_{\alpha\beta\gamma}^{543}/2 + iv\mathcal{P}_{\alpha\beta\gamma}^{355}(-\lambda^2c_\beta + \lambda\kappa s_\beta)/2 + \\
& + i(\sqrt{2}A_\kappa\kappa - 2v_S\kappa^2)\mathcal{P}_{\alpha\beta\gamma}^{522}/2 - i(\sqrt{2}A_\kappa\kappa + 6v_S\kappa^2)\mathcal{P}_{\alpha\beta\gamma}^{555}/6 - \\
& - iv\mathcal{P}_{\alpha\beta\gamma}^{322}(\lambda^2c_\beta + \lambda\kappa s_\beta)/2 + iv\mathcal{P}_{\alpha\beta\gamma}^{455}(\lambda\kappa c_\beta - \lambda^2s_\beta)/2 - \\
& - iv\mathcal{P}_{\alpha\beta\gamma}^{422}(\lambda\kappa c_\beta + \lambda^2s_\beta)/2 - iv(g_1^2 + g_2^2)c_{2\beta}\mathcal{P}_{\alpha\beta\gamma}^{411}s_\beta/8 - \\
& - i(g_1^2 + g_2^2)v c_\beta\mathcal{P}_{\alpha\beta\gamma}^{333}/8 - i(g_1^2 + g_2^2)v\mathcal{P}_{\alpha\beta\gamma}^{444}s_\beta/8 - \\
& - i\mathcal{P}_{\alpha\beta\gamma}^{511}(2v_S\lambda^2 + (\sqrt{2}A_\lambda\lambda + 2\kappa\lambda v_S)s_{2\beta})/2 + \\
& + ivc_\beta(-2\lambda^2 + (g_1^2 + g_2^2 - 2\lambda^2)c_{2\beta})\mathcal{P}_{\alpha\beta\gamma}^{311}/8 - \\
& - iv_S\lambda^2\mathcal{P}_{\alpha\beta\gamma}^{544}/2 - iv_S\lambda^2\mathcal{P}_{\alpha\beta\gamma}^{533}/2 + \\
& + i(\lambda\kappa)v\mathcal{P}_{\alpha\beta\gamma}^{521}.
\end{aligned}$$

Where \mathcal{P} is an abbreviation for the permutations of the Higgs rotation matrix elements, which are defined in Eq. 3.28

$$\begin{aligned}
\mathcal{P}_{\alpha\beta\delta}^{lmn} = & + \mathcal{R}_{\alpha n}\mathcal{R}_{\beta m}\mathcal{R}_{\delta l} + \mathcal{R}_{\alpha m}\mathcal{R}_{\beta n}\mathcal{R}_{\delta l} + \mathcal{R}_{\alpha n}\mathcal{R}_{\beta l}\mathcal{R}_{\delta m} + \\
& + \mathcal{R}_{\alpha l}\mathcal{R}_{\beta n}\mathcal{R}_{\delta m} + \mathcal{R}_{\alpha m}\mathcal{R}_{\beta l}\mathcal{R}_{\delta n} + \mathcal{R}_{\alpha l}\mathcal{R}_{\beta m}\mathcal{R}_{\delta n}.
\end{aligned}$$

APPENDIX B

The Decay Width

In Eq. (5.35), we have derived the amplitude $\mathcal{A}_{\alpha\beta\gamma}^{\text{nl0}}$ of the one-loop corrected $\mathbf{h}_\alpha \rightarrow \mathbf{h}_\beta \mathbf{h}_\gamma$ decay for the special case of $\alpha \in \{1, 2, 3\}$, $\beta, \gamma \in \{4, 5\}$. For the phenomenological discussion, the decay amplitude is used to determine the partial decay width $\Gamma_{\text{i}\rightarrow\text{f}}$, which, on the other hand, can also be derived from the in principle experimentally observable branching ratios and total width. The partial decay width of a particle of mass m decaying into n final state particles can be expressed in the rest frame of the decaying particle as,

$$d\Gamma = \frac{(2\pi)^2}{2m} |\mathcal{A}|^2 d\Phi_n(P; p_1, \dots, p_n). \quad (\text{B.1})$$

Where P is the four-momentum of the decaying particle, $P = (m, 0)$, and $d\Phi_n$ is the differential of the n particle phase space,

$$d\Phi_n(P; p_1, \dots, p_n) = \delta^4(P - \sum_{i=1}^n p_i) \prod_{i=1}^n \frac{d^3 p_i}{(2\pi)^3 2E_i}. \quad (\text{B.2})$$

In our special case of a $1 \rightarrow 2$ decay, the phase space can be integrated resulting in the specific form,

$$\Gamma_{\mathbf{h}_\alpha \rightarrow \mathbf{h}_\beta \mathbf{h}_\gamma}^{\text{nl0}} = \frac{\lambda^{1/2}(m_{\mathbf{h}_\alpha}^2, m_{\mathbf{h}_\beta}^2, m_{\mathbf{h}_\gamma}^2)}{16\pi m_{\mathbf{h}_\alpha}^3} |\mathcal{A}_{\alpha\beta\gamma}^{\text{nl0}}|^2, \quad (\text{B.3})$$

$$\text{with } \lambda^{1/2}(x, y, z) = \sqrt{x^2 - 2xy - 2xz - 2yz + y^2 + z^2}. \quad (\text{B.4})$$

In addition to the one-loop corrected decay width, for reasons of comparison we define the improved tree-level width, in which the matrix element \mathcal{A} is replaced by the mass corrected trilinear Higgs self-coupling $\bar{g}_{\alpha\beta\gamma}^{3\text{h}}$ according to Eq. (5.33)

$$\Gamma_{\mathbf{h}_\alpha \rightarrow \mathbf{h}_\beta \mathbf{h}_\gamma}^{\text{imp.tree}} = \frac{\lambda^{1/2}(m_{\mathbf{h}_\alpha}^2, m_{\mathbf{h}_\beta}^2, m_{\mathbf{h}_\gamma}^2)}{16\pi m_{\mathbf{h}_\alpha}^3} |\bar{g}_{\alpha\beta\gamma}^{3\text{h}}|^2 \quad (\text{B.5})$$

References

- [1] **ATLAS Collaboration, CMS Collaboration** Collaboration, I. Tsukerman, *Discovery potential at the LHC: Channels relevant for SM Higgs*. [arXiv:0812.1458](https://arxiv.org/abs/0812.1458) [hep-ex].
- [2] A. Djouadi, *The Anatomy of electro-weak symmetry breaking. I: The Higgs boson in the standard model*. Phys.Rept. **457** (2008) 1–216, [arXiv:hep-ph/0503172](https://arxiv.org/abs/hep-ph/0503172) [hep-ph].
- [3] M. Gell-Mann, *A schematic model of baryons and mesons*. Physics Letters **8** (1964) no. 3, 214 – 215. <http://www.sciencedirect.com/science/article/pii/S0031916364920013>.
- [4] G. Zweig, *An SU_3 model for strong interaction symmetry and its breaking*. *oai:cds.cern.ch:352337; Part I*.
- [5] S. L. Glashow, *Partial-symmetries of weak interactions*. Nuclear Physics **22** (1961) no. 4, 579 – 588. <http://www.sciencedirect.com/science/article/pii/0029558261904692>.
- [6] S. Weinberg, *A Model of Leptons* Phys. Rev. Lett. **19** (Nov, 1967) 1264–1266. <http://link.aps.org/doi/10.1103/PhysRevLett.19.1264>.
- [7] P. Higgs, *Broken symmetries, massless particles and gauge fields*. Physics Letters **12** (1964) no. 2, 132 – 133. <http://www.sciencedirect.com/science/article/pii/0031916364911369>.
- [8] P. W. Higgs, *Broken Symmetries and the Masses of Gauge Bosons* Phys. Rev. Lett. **13** (Oct, 1964) 508–509. <http://link.aps.org/doi/10.1103/PhysRevLett.13.508>.
- [9] F. Englert and R. Brout, *Broken Symmetry and the Mass of Gauge Vector Mesons* Phys. Rev. Lett. **13** (Aug, 1964) 321–323. <http://link.aps.org/doi/10.1103/PhysRevLett.13.321>.
- [10] T. W. B. Kibble, *Symmetry Breaking in Non-Abelian Gauge Theories* Phys. Rev. **155** (Mar, 1967) 1554–1561. <http://link.aps.org/doi/10.1103/PhysRev.155.1554>.
- [11] A. Sakharov, *Violation of CP Invariance, c Asymmetry, and Baryon Asymmetry of the Universe*. Reprinted in *Kolb, E.W. (ed.), Turner, M.S. (ed.): The early universe* 371-373, and in *Lindley, D. (ed.) et al.: Cosmology and particle physics* 106-109, and in Sov. Phys. Usp. 34 (1991) 392-393 [Usp. Fiz. Nauk 161 (1991) No. 5 61-64].
- [12] J. Wess and B. Zumino, *Supergauge transformations in four dimensions*. Nuclear Physics B **70** (1974) no. 1, 39 – 50. <http://www.sciencedirect.com/science/article/pii/0550321374903551>.

- [13] P. Fayet, *Supersymmetry and weak, electromagnetic and strong interactions*. Physics Letters B **64** (1976) no. 2, 159 – 162.
<http://www.sciencedirect.com/science/article/pii/0370269376903191>.
- [14] P. Fayet, *Spontaneously broken supersymmetric theories of weak, electromagnetic and strong interactions*. Physics Letters B **69** (1977) no. 4, 489 – 494.
<http://www.sciencedirect.com/science/article/pii/0370269377908528>.
- [15] M. F. Sohnius, *Introducing supersymmetry*. Physics Reports **128** (1985) no. 2–3, 39 – 204.
<http://www.sciencedirect.com/science/article/pii/0370157385900237>.
- [16] R. Haag, J. T. Łopuszański, and M. Sohnius, *All possible generators of supersymmetries of the S-matrix*. Nuclear Physics B **88** (1975) no. 2, 257 – 274.
<http://www.sciencedirect.com/science/article/pii/0550321375902795>.
- [17] S. P. Martin, *A Supersymmetry primer*. arXiv:hep-ph/9709356 [hep-ph].
- [18] A. Djouadi, *The Anatomy of electro-weak symmetry breaking. II. The Higgs bosons in the minimal supersymmetric model*. Phys.Rept. **459** (2008) 1–241,
arXiv:hep-ph/0503173 [hep-ph].
- [19] S. Dawson, *The MSSM and why it works*. arXiv:hep-ph/9712464 [hep-ph].
- [20] **ALEPH Collaboration, DELPHI Collaboration, L3 Collaboration, OPAL Collaboration** Collaboration, A. Sopczak, *MSSM Higgs boson searches at LEP*. arXiv:hep-ph/0602136 [hep-ph].
- [21] J. E. Kim and H. Nilles, *The μ -problem and the strong CP-problem*. Physics Letters B **138** (1984) no. 1–3, 150 – 154.
<http://www.sciencedirect.com/science/article/pii/0370269384918902>.
- [22] U. Ellwanger, C. Hugonie, and A. M. Teixeira, *The Next-to-Minimal Supersymmetric Standard Model*. Phys.Rept. **496** (2010) 1–77, arXiv:0910.1785 [hep-ph].
- [23] J. Ellis, J. F. Gunion, H. E. Haber, L. Roszkowski, and F. Zwirner, *Higgs bosons in a nonminimal supersymmetric model* Phys. Rev. D **39** (Feb, 1989) 844–869.
<http://link.aps.org/doi/10.1103/PhysRevD.39.844>.
- [24] U. Ellwanger, M. Rausch de Traubenberg, and C. A. Savoy, *Phenomenology of supersymmetric models with a singlet*. Nucl.Phys. **B492** (1997) 21–50,
arXiv:hep-ph/9611251 [hep-ph].
- [25] M. Maniatis, *The Next-to-Minimal Supersymmetric extension of the Standard Model reviewed*. Int. J. Mod. Phys. **A25** (2010) 3505–3602, arXiv:0906.0777 [hep-ph].
- [26] S. Abel and P. White, *Baryogenesis from domain walls in the next-to-minimal supersymmetric standard model*. Phys.Rev. **D52** (1995) 4371–4379,
arXiv:hep-ph/9505241 [hep-ph].
- [27] L. Girardello and M. Grisaru, *Soft breaking of supersymmetry*. Nuclear Physics B **194** (1982) no. 1, 65 – 76.
<http://www.sciencedirect.com/science/article/pii/0550321382905120>.
- [28] R. Feynman, *Space - time approach to quantum electrodynamics*. Phys.Rev. **76** (1949) 769–789.
- [29] J. Collins, *Renormalization: An Introduction to Renormalization, the Renormalization Group, and the Operator-product Expansion*. Cambridge Monographs on Mathematical Physics. Cambridge University Press, 1986.

- [30] P. A. M. Dirac, *Directions in physics: lectures delivered during a visit to Australia and New Zealand, August/ September 1975*. A Wiley-Interscience publication. Wiley, New York, c 1978.
- [31] R. P. Feynman, *QED: the strange theory of light and matter*. Alix G. Mautner memorial lectures. Univ. Pr., Princeton, NJ, 1985.
- [32] G. 't Hooft and M. J. G. Veltman, *Regularization and Renormalization of Gauge Fields*. Nucl. Phys. **B44** (1972) 189–213.
- [33] W. Siegel, *Supersymmetric dimensional regularization via dimensional reduction*. Physics Letters B **84** (1979) no. 2, 193 – 196.
<http://www.sciencedirect.com/science/article/pii/037026937990282X>.
- [34] T. Hahn and M. Perez-Victoria, *Automatized one loop calculations in four-dimensions and D-dimensions*. Comput.Phys.Commun. **118** (1999) 153–165, [arXiv:hep-ph/9807565](https://arxiv.org/abs/hep-ph/9807565) [hep-ph].
- [35] F. del Aguila, A. Culatti, R. Munoz Tapia, and M. Perez-Victoria, *Techniques for one loop calculations in constrained differential renormalization*. Nucl.Phys. **B537** (1999) 561–585, [arXiv:hep-ph/9806451](https://arxiv.org/abs/hep-ph/9806451) [hep-ph].
- [36] T. Hahn, *Generating Feynman diagrams and amplitudes with FeynArts 3*. Comput.Phys.Commun. **140** (2001) 418–431, [arXiv:hep-ph/0012260](https://arxiv.org/abs/hep-ph/0012260) [hep-ph].
- [37] J. A. M. Vermaseren, *New features of FORM* ArXiv Mathematical Physics e-prints (Oct., 2000) , [arXiv:math-ph/0010025](https://arxiv.org/abs/math-ph/0010025).
- [38] F. Staub, *From Superpotential to Model Files for FeynArts and CalcHep/CompHep*. Comput.Phys.Commun. **181** (2010) 1077–1086, [arXiv:0909.2863](https://arxiv.org/abs/0909.2863) [hep-ph].
- [39] K. Walz, *Analysis of the Higgs Boson Masses at One-Loop Level in the Complex NMSSM*, 2011.
- [40] K. Ender, T. Graf, M. Muhlleitner, and H. Rzehak, *Analysis of the NMSSM Higgs Boson Masses at One-Loop Level*. Phys.Rev. **D85** (2012) 075024, [arXiv:1111.4952](https://arxiv.org/abs/1111.4952) [hep-ph].
- [41] A. Denner, *Techniques for calculation of electroweak radiative corrections at the one loop level and results for W physics at LEP-200*. Fortsch.Phys. **41** (1993) 307–420, [arXiv:0709.1075](https://arxiv.org/abs/0709.1075) [hep-ph].
- [42] P. H. Chankowski, S. Pokorski, and J. Rosiek, *One loop corrections to the supersymmetric Higgs boson couplings and LEP phenomenology*. Phys.Lett. **B286** (1992) 307–314.
- [43] G. Degrandi and P. Slavich, *On the radiative corrections to the neutral Higgs boson masses in the NMSSM*. Nucl.Phys. **B825** (2010) 119–150, [arXiv:0907.4682](https://arxiv.org/abs/0907.4682) [hep-ph].
- [44] U. Ellwanger, J. F. Gunion, and C. Hugonie, *Establishing a no lose theorem for NMSSM Higgs boson discovery at the LHC*. [arXiv:hep-ph/0111179](https://arxiv.org/abs/hep-ph/0111179) [hep-ph].
- [45] U. Ellwanger, J. F. Gunion, C. Hugonie, and S. Moretti, *Towards a no lose theorem for NMSSM Higgs discovery at the LHC*. [arXiv:hep-ph/0305109](https://arxiv.org/abs/hep-ph/0305109) [hep-ph].
- [46] M. Almarashi and S. Moretti, *Reinforcing the no-lose theorem for NMSSM Higgs discovery at the LHC*. Phys.Rev. **D84** (2011) 035009, [arXiv:1106.1599](https://arxiv.org/abs/1106.1599) [hep-ph].

- [47] **ATLAS Collaboration** Collaboration, G. Aad *et al.*, *Combined search for the Standard Model Higgs boson using up to 4.9 fb⁻¹ of pp collision data at sqrt(s) = 7 TeV with the ATLAS detector at the LHC*. Phys.Lett. **B710** (2012) 49–66, [arXiv:1202.1408](#) [hep-ex].
- [48] **CMS Collaboration** Collaboration, S. Chatrchyan *et al.*, *Combined results of searches for the standard model Higgs boson in pp collisions at sqrt(s) = 7 TeV*. Phys.Lett. **B710** (2012) 26–48, [arXiv:1202.1488](#) [hep-ex].
- [49] S. King, M. Muhlleitner, and R. Nevzorov, *NMSSM Higgs Benchmarks Near 125 GeV*. Nucl.Phys. **B860** (2012) 207–244, [arXiv:1201.2671](#) [hep-ph].
- [50] P. Z. Skands, B. Allanach, H. Baer, C. Balazs, G. Belanger, *et al.*, *SUSY Les Houches accord: Interfacing SUSY spectrum calculators, decay packages, and event generators*. JHEP **0407** (2004) 036, [arXiv:hep-ph/0311123](#) [hep-ph].
- [51] B. Allanach, C. Balazs, G. Belanger, M. Bernhardt, F. Boudjema, *et al.*, *SUSY Les Houches Accord 2*. Comput.Phys.Commun. **180** (2009) 8–25, [arXiv:0801.0045](#) [hep-ph].
- [52] **ATLAS Collaboration** Collaboration, G. Aad *et al.*, *Search for squarks and gluinos using final states with jets and missing transverse momentum with the ATLAS detector in sqrt(s) = 7 TeV proton-proton collisions*. Phys.Lett. **B710** (2012) 67–85, [arXiv:1109.6572](#) [hep-ex].
- [53] **CMS Collaboration** Collaboration, S. Chatrchyan *et al.*, *Search for Supersymmetry at the LHC in Events with Jets and Missing Transverse Energy*. Phys.Rev.Lett. **107** (2011) 221804, [arXiv:1109.2352](#) [hep-ex].
- [54] A. Djouadi, J. Kalinowski, and M. Spira, *HDECAY: A Program for Higgs boson decays in the standard model and its supersymmetric extension*. Comput.Phys.Commun. **108** (1998) 56–74, [arXiv:hep-ph/9704448](#) [hep-ph].
- [55] J. Butterworth, F. Maltoni, F. Moortgat, P. Richardson, S. Schumann, *et al.*, *The Tools and Monte Carlo working group Summary Report*. [arXiv:1003.1643](#) [hep-ph].
- [56] P. Bechtle, O. Brein, S. Heinemeyer, G. Weiglein, and K. E. Williams, *Introducing HiggsBounds 2.0.0*. PoS **CHARGED2010** (2010) 027, [arXiv:1012.5170](#) [hep-ph].
- [57] **OPAL Collaboration** Collaboration, G. Abbiendi *et al.*, *Search for invisibly decaying Higgs bosons in e+ e- -> Z0 h0 production at sqrt(s) = 183 GeV - 209 GeV*. Phys.Lett. **B682** (2010) 381–390, [arXiv:0707.0373](#) [hep-ex].
- [58] **ALEPH Collaboration, DELPHI Collaboration, L3 Collaboration, OPAL Collaborations, LEP Working Group for Higgs Boson Searches Collaboration**, S. Schael *et al.*, *Search for neutral MSSM Higgs bosons at LEP*. Eur.Phys.J. **C47** (2006) 547–587, [arXiv:hep-ex/0602042](#) [hep-ex].

Danksagung

An erster Stelle möchte ich mich bei Prof. Margarete Mühlleitner für die Gelegenheit bedanken, meine Diplomarbeit in diesem gleichermaßen interessanten wie herausfordernden Themengebiet anfertigen zu können. Unsere regelmäßigen Gespräche in der Anfangsphase und die unzähligen Korrekturvorschläge bei der Fertigstellung dieser Arbeit haben mir sehr weiter geholfen.

Herrn Prof. Matthias Steinhauser gilt mein Dank für die Übernahme des Korreferats.

Bei Dr. Thi Nhung Dao und Kathrin Walz möchte ich mich für den hilfreichen Austausch und für die Vergleichsmöglichkeiten meiner Berechnungen bedanken. Kathrin danke ich des Weiteren auch für die vielen hilfreichen Tipps und dass sie so häufig dazu beigetragen hat, meine Unklarheiten zu beseitigen.

Zu danken habe ich auch dem gesamten Institut für die entspannte und gleichzeitig produktive Atmosphäre, namentlich möchte ich noch Yasmin Anstruther, Johannes Bellm und Matthias Weinreuter für das Korrekturlesen einzelner Kapitel danken.

Zu guter letzt sei an dieser Stelle meinen Freunden gedankt, meinen Eltern, die mich Zeit meines Lebens mit Rat und Tat unterstützen, sowie meiner Jenny für ihre Liebe und Unterstützung in allen Lebenslagen.